

Simultaneous Screening of Multiple Substrates with an Unspecific Peroxygenase Enabled Modified Alkane and Alkene Oxyfunctionalisations

Anja Knorrscheidt,^a Jordi Soler,^c Nicole Hünecke,^a Pascal Püllmann,^a Marc Garcia-Borràs*^c and Martin J. Weissenborn*^{a, b}

-
- a Bioorganic Chemistry
Leibniz Institute of Plant Biochemistry
Weinberg 3, 06120 Halle (Saale), Germany
E-mail: martin.weissenborn@ipb-halle.de
- b Jun.-Prof. Martin J. Weissenborn
Institute of Chemistry
Martin Luther University Halle-Wittenberg
Kurt-Mothes-Str. 2, 06120 Halle (Saale), Germany
- c Institut de Química Computacional i Catàlisi and Departament de Química
Universitat de Girona
Carrer Maria Aurèlia Capmany 69
Girona 17003, Catalonia, Spain

Table of contents

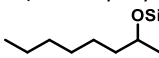
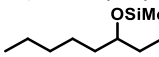
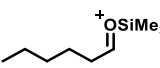
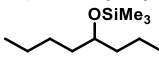
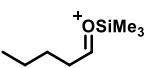
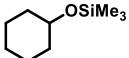
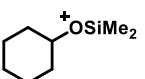
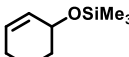
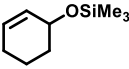
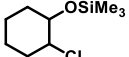
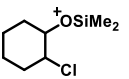
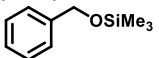
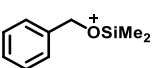
1. General information.....	2
2. MISER-GC-MS method validation.....	6
3. Mutagenesis of <i>Mth</i> UPO and screening procedure.....	8
4. Product quantification.....	10
5. Computational details.....	18
6. References.....	13

1. General information

Chemicals. Solvents were used as provided without further purification from Carl Roth (Karlsruhe, DE) as GC ultra-grade. The commercially available compounds were also used without further purification from the following suppliers: hydrogen peroxide solution (30 % (w/w) in H₂O, Sigma-Aldrich, St. Louis, US), styrene (99 % contains 4-*tert*-butylcatechol, Sigma-Aldrich, St. Louis, US), *n*-octane (97 %, TCI, Tokyo, JP), 1-octanol (99.5 %, Fluka, Buchs, CH), 2-octanol (98 %, TCI, Tokyo, JP), 3-octanol (98 %, TCI, Tokyo, JP), 4-octanol (97, Sigma-Aldrich, St. Louis, US), cyclohexane (99, Sigma-Aldrich, St. Louis, US), cyclohexene (99.5, Fluka, Buchs, CH), 1,2-epoxycyclohexane (98, TCI, Tokyo, JP), 2-chlorocyclohexanol (90, Sigma-Aldrich, St. Louis, US), 2-cyclohexen-1-ol (95, Fluka, Buchs, CH), cyclohexanol (99, Sigma-Aldrich, St. Louis, US), 1-methyl-1-cyclohexene (98, TCI, Tokyo, JP), *cis*- β -methylstyrene (98, TCI, Tokyo, JP), styrene oxide (98, TCI, Tokyo, JP), (*R*)-styrene oxide (97 %, Sigma-Aldrich, St. Louis, US), α -methylstyrene (99 %, stabilised with 10-20 4-*tert*-butylcatechol, Alfa Aesar, Karlsruhe, DE), *N*-trimethylsilylimidazole (98 %, TCI, Tokyo, JP), cinnamic aldehyde (95 %, Sigma-Aldrich, St. Louis, US), cinnamic alcohol (97 %, Sigma-Aldrich, St. Louis, US) and benzyl alcohol (99 %, Sigma-Aldrich, St. Louis, US). As a buffer system, 50 mM potassium phosphate (KPi) pH 7.0 was utilised as an aqueous phase for the bioconversions.

Multiple injection in a single chromatographical run for gas chromatography–mass spectrometry (MISER-GC-MS). Measurements were performed on a Shimadzu GCMS-QP2010 Ultra (Shimadzu, Kyoto, JP) with an OPTIMA 5MS Accent column (25 m x 0.20 mm, 0.20 μ m film, Macherey-Nagel, DE) and helium as carrier gas. The injection volume was set to 1 μ l of each sample and within the liner a split ratio of 1:60 was adjusted. The injection temperature was 280 °C with a linear velocity control of 59.7 cm/sec. The samples were injected every 33 seconds under an isothermal oven temperature of 190 °C which was hold for 60 minutes. To avoid column contaminations, the columns was additionally heated for 30 minutes at 300 °C. The following temperature in the MS were adjusted: 250 °C for the ion source and 290 °C for the interface. The selected ion monitoring (SIM) mode was applied to filter out only the corresponding *m/z* traces as depicted in Tab. S1.

Tab. S1 Overview of the utilised compounds and their *m/z* traces for the MISER-GC-MS approach.

#	Compound	Utilised <i>m/z</i> trace for the MISER-GC-MS analysis
1	O-(trimethylsilyl)-2-octanol 	117 = 
2	O-(trimethylsilyl)-3-octanol 	173 = 
3	O-(trimethylsilyl)-4-octanol 	159 = 
4	O-(trimethylsilyl)-cyclohexanol 	157 = 
5	O-(trimethylsilyl)-2-cyclohexen-1-ol 	170 = main mass 
6	O-(trimethylsilyl)-2-chlorocyclohexanol 	191 = 
7	O-(trimethylsilyl)-phenylmethanol 	165 = 

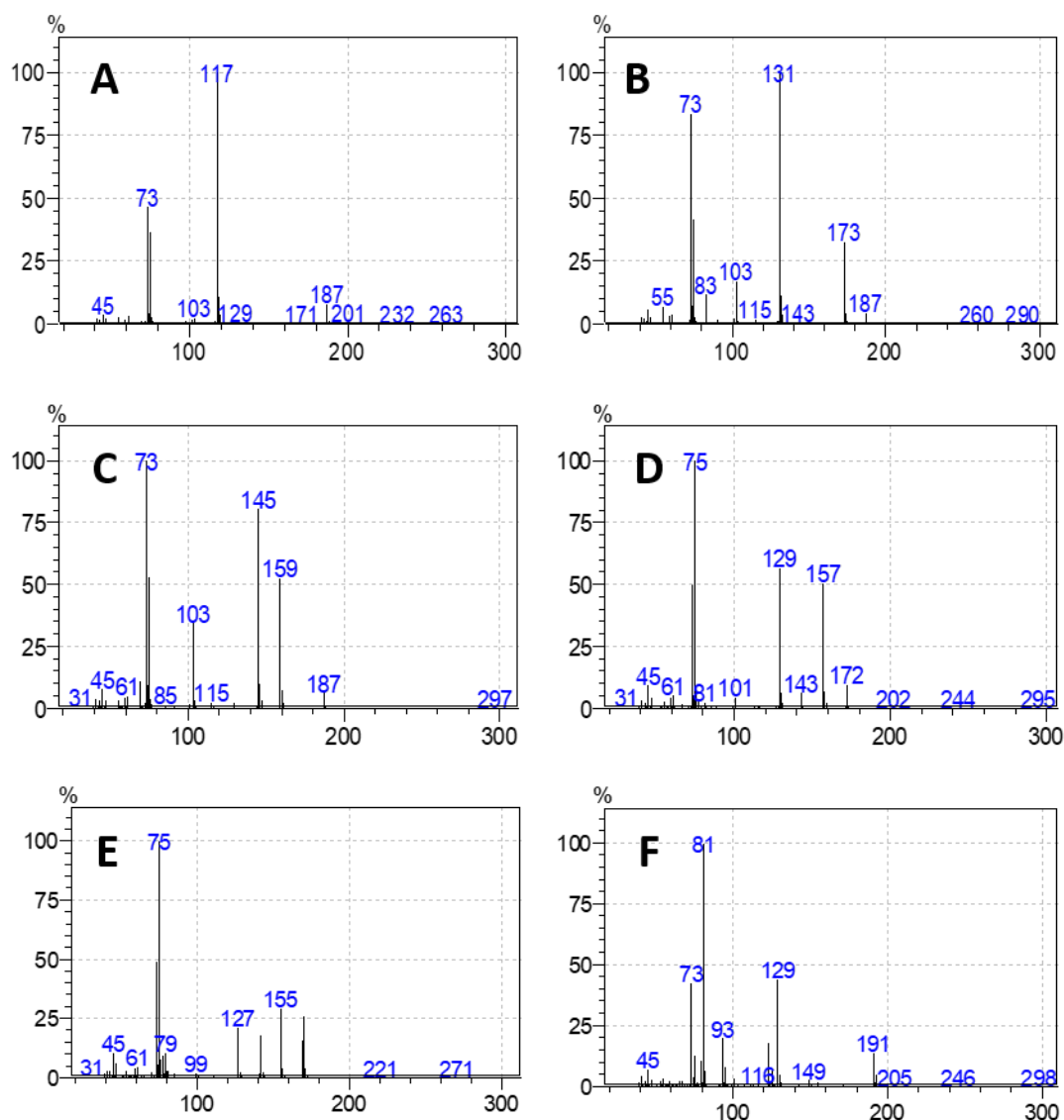


Fig. S1 Fragmentation pattern of silylated A) 2-octanol, C) 3-octanol, D) 4-octanol, E) cyclohexanol and F) 2-chlorocyclohexanol by electron impact ionisation.

Single gas chromatography measurements. Measurements were performed on a Shimadzu GCMS-QP2020 NX instrument (Shimadzu, Kyoto, JP) with a SH-Rxi-5Sil MS column (30 m x 0.25 mm, Shimadzu, Kyoto, JP) for achiral measurements, whereas helium was utilised as the carrier gas. The samples were injected splitless (1 μ l) with a liner temperature of 280 $^{\circ}$ C (expectations bioconversion of styrene, *cis*- β -methylstyrene, α -methylstyrene: 180 $^{\circ}$ C). The interface temperature was set to 290 $^{\circ}$ C. Ionisation was obtained by electron impact with a voltage of 70 V, and the temperature of the ion source was 250 $^{\circ}$ C. The oven temperature profile for each compound is shown in table S2. The detector voltage of the secondary electron multiplier was adjusted in relation to the tuning results with perfluorotributylamine. The GC-MS parameters were controlled with GCMS Real Time Analysis, and for data evaluation, GCMS Postrun Analysis (GCMSsolution Version 4.45, Shimadzu, Kyoto, JP) was used. Calibration and quantification were implemented in scan mode by filtering out the corresponding *m/z* trace (Tab. S2).

Tab. S2 Instrumental parameters for GC-MS single measurements.

Products	GC-MS	Column	Temperature program
1-octanol (<i>m/z</i> 41)	Achiral	SH-Rxi-5Sil MS	40 °C
2-octanol (<i>m/z</i> 45)			7 °C/min to 110 °C
3-octanol (<i>m/z</i> 59)			100 °C/min to 300 °C hold 1 min
4-octanol (<i>m/z</i> 69)			(solvent cut: 7 min)
Styrene oxide (<i>m/z</i> 120)	Achiral	SH-Rxi-5Sil MS	40 °C
			7 °C/min to 130 °C
			100 °C/min to 300 °C hold 1 min
			(solvent cut: 8 min, injection temperature: 100 °C)
	Chiral	Lipodex E	80 °C hold 30 min
			50 °C/min to 200 °C hold 5 min
			(solvent cut: 9 min, injection temperature: 180 °C)
α -methylstyrene oxide (<i>m/z</i> : TCI, calibrated with TCI of styrene oxide)	Achiral	SH-Rxi-5Sil MS	40 °C
			7 °C/min to 130 °C
			100 °C/min to 300 °C hold 1 min
			(solvent cut: 4 min, injection temperature: 180 °C)
α -methylstyrene oxide (<i>m/z</i> 133)	Chiral	Lipodex E	60 °C hold 120 min
			5 °C/min to 120 °C
			50 °C/min to 200 °C hold 2 min
			(solvent cut: 9 min, injection temperature: 180 °C)
cinnamic aldehyde (<i>m/z</i> 131) cinnamic alcohol (<i>m/z</i> 134)	Achiral	SH-Rxi-5Sil MS	90 °C hold
			2 °C/min to 100 °C
			100 °C/min to 300 min hold 2 min
			(solvent cut: 13 min, injection temperature: 180 °C)
Cyclohexene oxide (<i>m/z</i> 83)	Achiral	SH-Rxi-5Sil MS	40 °C
			7 °C/min to 90 °C
			100 °C/min to 300 °C hold 1 min
			(solvent cut: 3 min)
1-Methylcyclohexene oxide (TCI, calibrated with TCI of cyclohexene oxide)	Chiral	Lipodex E	55 °C hold 15 min
			50 °C/min to 200 °C hold 2 min
			(solvent cut: 3 min)

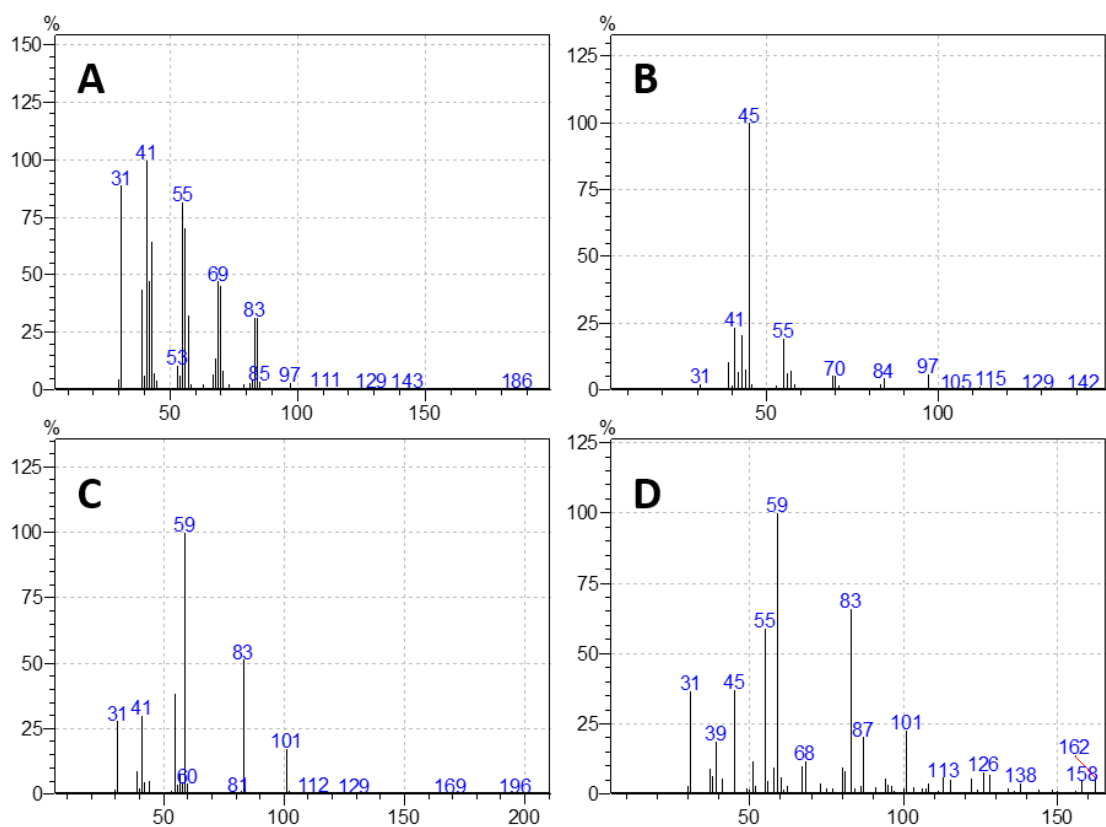


Fig. S2 Fragmentation pattern of A) 1-octanol, B) 2-octanol, C) 3-octanol and D) 4-octanol by electron impact ionisation.

2. MISER-GC-MS method validation

Verification of linearity in extraction and MS response. 400 μL of a 50 mM KPi buffer (pH 7.0) served as aqueous reaction model system. The corresponding products were solved in this aqueous system with help of 5 % (v/v) acetone in the following concentrations: 100/200/500 μM . The extraction was accomplished with pure *n*-hexane in triplicates for each concentration. For the ring opening of the epoxide product and for derivatisation the MUSE protocol was followed. The resulting linear response for the extraction as well as for the MS is illustrated in Fig S3.

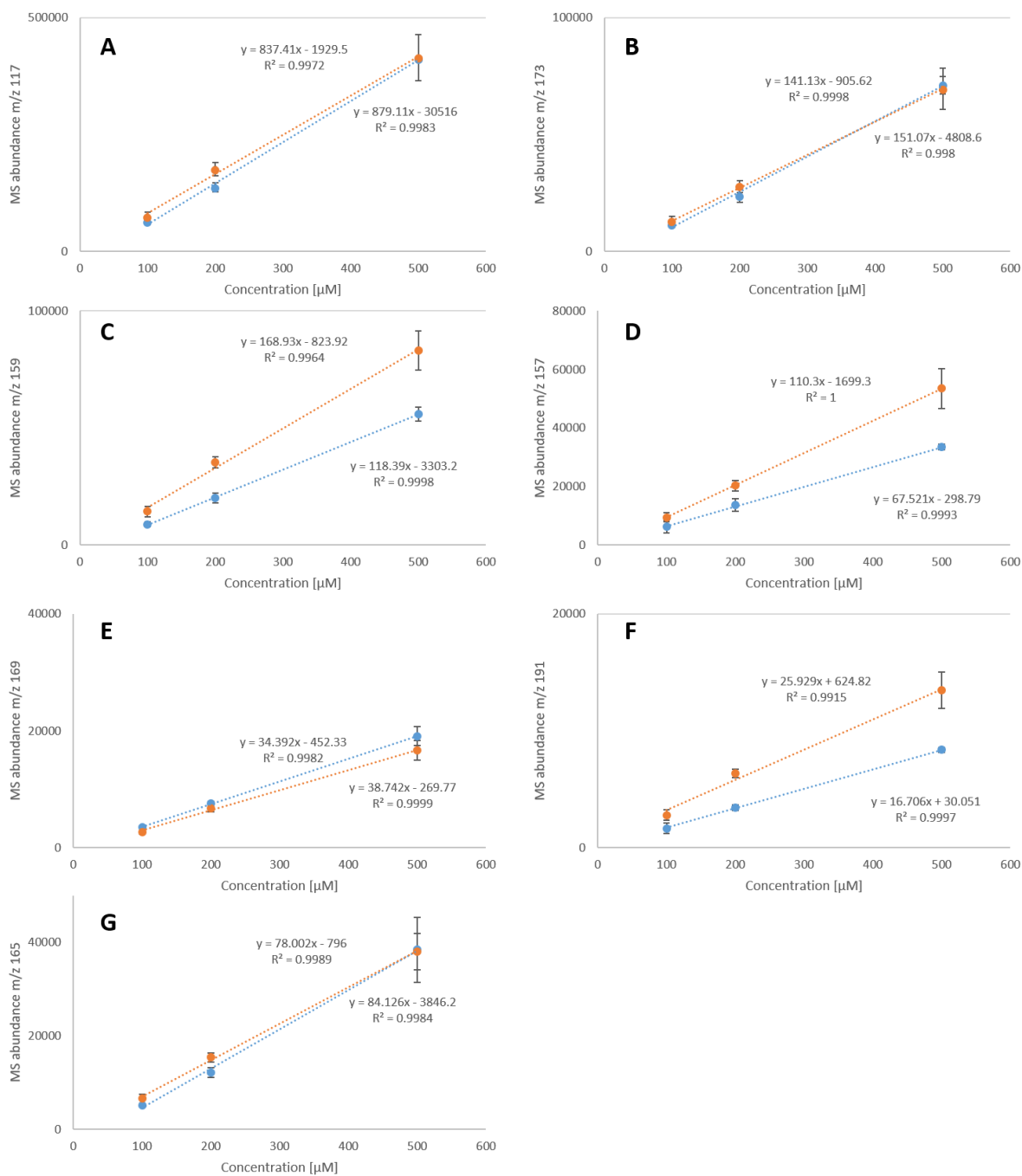


Fig. S3 Verification of linearity in extraction and MS response for single (blue) vs. multiple (orange) components: A) 2-octanol, B) 3-octanol, C) 4-octanol, D) cyclohexanol, E) cyclohexenol, F) 2-chlorocyclohexanol, G) benzyl alcohol.

Verification of 96 biological replicates within the multiple substrate assay. Before screening of whole variant libraries, the developed MISER-GC-MS approach with multiple substrates was tested for one whole microtiter plate including biological replicates of *MthUPO* wild type. *MthUPO* was cultivated and tested for the conversion of octane, cyclohexane and cyclohexene as described in the corresponding sections. The GC-MS results were shown in Tab. S3.

Tab. S3 Verification of one microtiter plate of *MthUPO* wildtype (96 biological replicates) for the multiple substrate screening with octane, cyclohexane and cyclohexene (as internal standard (IS) benzyl alcohol was utilised).

	Quotient (Product/IS)					
	2-octanol	3-octanol	4-octanol	cyclohexanol	2-cyclohexenol	2-chlorocyclohexanol
Quotient mean	0.03242	0.01230	0.01236	0.00219	0.00063	0.00593
Standard deviation	0.00400	0.00121	0.00093	0.00025	0.00007	0.00068
Standard deviation [%]	12.3	9.9	7.5	11.2	10.2	7.3

3. Mutagenesis of *MthUPO* and screening procedure

Single site saturation mutagenesis. Mutagenesis was performed using the Golden Mutagenesis technique¹ combined with the “22c-trick”² for residue randomisation. The *MthUPO* wild type gene combined with a *Sce*- α Galactosidase signal peptide at the *N*-terminus and a TwinStrep-GFP11 purification/detection tag at the *C*-terminus was chosen as genetic template¹ targeting the following amino acid residues within the active site or the entrance channel for randomisation: L56, F59, L60, L86, F154, T155, S159, A161, L206. As backbone structure, the expression plasmid pAGT572_Nemo 2.0 was utilised, enabling bacterial antibiotic selection (ampicillin/carbenicillin resistance) and yeast auxotrophy selection (URA3 marker). As a placeholder for the target gene sequence, a lacZ cassette (approx. 600 bp) is integrated, which enables β -galactosidase based blue/white selection of transformants based on the conversion of X-Gal. For the mutagenesis, the Golden Mutagenesis protocol was applied.^[1] The resulting Golden Gate setup mixture was transformed in chemically competent *E.coli* DH10B cells. After heat shock transformation (90 seconds at 42 °C) and recovery (1h at 37 °C) the mixture (approx. 320 μ L) was split into two fractions, 60 μ L were plated on selective LB agar plates (50 μ g \times mL⁻¹ X-Gal; 100 μ g \times mL⁻¹ carbenicillin; 150 μ M IPTG) and the remaining volume used to directly inoculate 4 mL TB Medium (100 μ g \times mL⁻¹ carbenicillin). The plasmid DNA mixture was isolated from the liquid culture using a NucleoSpin Plasmid Kit (Macherey-Nagel, Düren, DE). The efficiency of the Golden Gate reaction was evaluated based on the performed blue/white screening and the Golden Mutagenesis analysing feature “Quick Quality Control”³ monitoring the codon distribution at the previously mentioned positions. The resulting plasmid DNA mixture was then transformed into chemically competent yeast cells (INVSc1 strain) by polyethylene glycol/lithium acetate transformation. For transformation, an amount of 100 ng of the plasmid preparation was added to 10 μ L of salmon sperm DNA (10 mg/mL; Sigma Aldrich, Hamburg, DE) and mixed. This mixture was then added to a thawed aliquot of INVSc1 cells on ice. 600 μ L of transformation buffer (40 % (v/v) polyethylene glycol 4000; 100 mM lithium acetate; 1 mM EDTA; 10 mM Tris-HCl pH 7.4) were added and the cells incubated under rigid shaking (30 °C; 850 rpm) for 30 min. Afterwards, 70 μ L of pure DMSO were added and the cells incubated for a further 15 min at 42 °C without shaking. Finally, the cells were precipitated by short centrifugation, the supernatant discarded, and the cell pellet resuspended in 350 μ L sterile ddH₂O. Different volumes were plated on Synthetic Complement (SC) Drop Out plates supplemented with 2 % (w/v) glucose as carbon source and lacking Uracil as an auxotrophic selection marker. Plates were incubated for at least 48 hours at 30 °C till clearly background distinguishable white colonies appeared.¹

Microtiter plate cultivation of *S. cerevisiae*. For *Mth*UPO production in microtiter plate format specialised 96 half deep well plates were utilised. The model type CR1496c was purchased from EnzyScreen (Heemstede, NL) and plates were covered with fitting CR1396b Sandwich cover for cultivation. Plates and covers were flushed before every experiment thoroughly with 70 % ethanol and air-dried under a sterile bench until usage. In each cavity, 220 μ L of minimal expression medium were filled and inoculated with single, clearly separated yeast colonies using sterile toothpicks. The minimal selective expression medium (1x concentrated SC Drop stock solution lacking uracil, 2 % (w/v) galactose, 71 mM potassium phosphate buffer pH 6.0, 3.2 mM magnesium sulfate, 3.3 % (v/v) ethanol, 50 mg/L haemoglobin, 25 mg/L chloramphenicol) was freshly prepared out of sterile stock solutions immediately before each experiment, mixed and added to the cavities. After inoculation of the wells the plates were covered, mounted on CR1800 cover clamps (EnzyScreen) and incubated in a Minitron shaking incubator (Infors, Bottmingen, SUI) for 72 h (30 °C; 230 rpm). After cultivation, the cells were separated from the peroxygenase containing supernatant by centrifugation (3400 rpm; 45 min; 4 °C).¹ The cell pellet was resuspended in the remaining supernatant, and glycerol was added to achieve a final concentration of 25 % (v/v). The sealed microtiter plate was frozen by liquid nitrogen and stored at – 80 °C as mother plate for subsequent hit verification.

Multiple substrate protocol for hydroxylation of octane, cyclohexane, cyclohexene. For the reaction stock solutions were prepared and utilised: the alkane mix contained 100 mM octane, 100 mM cyclohexane and 100 mM cyclohexene in acetone and the H₂O₂ stock contained 20 mM H₂O₂ in KPi buffer (100 mM, pH 7.0). 100 μ L of the supernatant containing the corresponding *Mth*UPO variant was transferred from the cultivation plate to a deep-well EnzyScreen plate. To the supernatant 260 μ L KPi buffer (100 mM, pH 7.0), 20 μ L of alkane stock and 20 μ L of the H₂O₂ stock was added. The reaction was performed at 25 °C and 300 rpm for one hour. For the epoxide ring opening, 10 μ L concentrated HCl was added to each well, followed by 30 minutes of reaction time at 300 rpm and 25 °C. For the extraction, the extraction solution was always prepared freshly containing 250 μ M benzyl alcohol in *n*-hexane. 500 μ L of the extraction solution was added and the extraction was accomplished by shaking the microtiter plate at 300 rpm and 25 °C for 30 minutes. 200 μ L of the organic layer was transferred to another deep-well EnzyScreen plate and additional 400 μ L of the extraction solution was added. To start the silylation 2.5 μ L of *N*-trimethylsilylimidazole was added and the silylation was conducted for additional 30 minutes at 25 °C at 300 rpm. The formed imidazole had to be washed out before loading the samples to the GC-MS. Therefore, 400 μ L of water were added to the silylation reaction and the washing was achieved by 300 rpm at 25 °C for 30 minutes. For the GC-MS measurement at least 300 μ L were transferred to a glass-coated microtiter plate and was analysed by the previous described MISER-GC-MS method. Hits were verified by rescreening in triplicates under the same reaction conditions with direct extraction by *n*-hexane (containing 250 μ M benzyl alcohol) in single GC-MS measurements.

Shake flask cultivation and protein purification. For the preculture 50 mL of SC Drop out selection media (+ 2 % (w/v) Raffinose as non-repressible carbon source and 25 mg/L chloramphenicol) was inoculated with one single colony derived from a selection plate (SC Drop; -Uracil) and grown for 48 h (30 °C; 160 rpm; 80 % humidity). The main expression culture was inoculated with a starting optical density of 0.3. For large scale peroxygenase production rich non-selective expression medium (20 g/L peptone; 10 g/L yeast extract; 2 % (w/v) galactose; 71 mM potassium phosphate buffer pH 6.0; 3.2 mM magnesium sulfate; 3.3 % (v/v) ethanol; 25 mg/L chloramphenicol) was utilised. Cultivation was performed in 2.5 L Ultra yield flasks (Thomson Instrument, Oceanside, US) in a final culture volume of 500 mL per flask after sealing the flask with breathable Aeraseal tape (Sigma Aldrich, Hamburg, DE) allowing for gas exchange. The main cultures were incubated for further 72 h (25 °C; 110 rpm). After cultivation, the cells were separated from the peroxygenase containing supernatant by centrifugation

(4300 rpm; 35 min; 4 °C). The supernatant was concentrated approx. 10-fold using ultrafiltration. Therefore, a Sartocoon Slice 200 membrane holder (Sartorius, Göttingen, DE) was equipped with a Sartocoon Slice 200 ECO Hydrosart Membrane (10 kDa nominal cut-off; Sartorius) within a self-made flow setup. The flow system for ultrafiltration was operated by an EasyLoad peristaltic pump (VWR International, Darmstadt, DE). The cleared supernatant (500 mL) was concentrated to a volume of 50 mL, and 900 mL of purification binding buffer (100 mM Tris-HCl pH 8.0, 150 mM NaCl) were added as a buffer exchange step. This sample was then concentrated to a final volume of 50 mL. Protein purification was implemented utilising the C-terminal attached double Strep II Tag (WSHPQFEK), coined TwinStrep® (Iba Lifesciences, Göttingen, DE). As a column, Gravity Strep-Tactin®XT Superflow® columns (5 mL; Iba Lifesciences) were chosen. In the first step, the column was equilibrated with 5 column volumes (CVs) binding buffer. The concentrated sample (50 mL) was filter sterilised (0.2 µm syringe filter) and applied to the column. After application, the column was washed with 6 CVs binding buffer. Elution was performed based on binding competition with biotin, therefore approx. 2 CV of elution buffer (100 mM Tris-HCl pH 8.0, 150 mM NaCl; 50 mM biotin) were applied to the column. The pooled elution fraction was then dialysed overnight (4 °C) against 5 L of storage buffer (100 mM potassium phosphate pH 7.0) using ZelluTrans dialysis tubing (6-8 kDa nominal cut-off; Carl Roth).¹ The enzyme concentration of the dialysed samples was determined by colourimetric BCA assay utilising a Pierce™ BCA Protein Assay Kit (ThermoFisherScientific, Waltham, US) following the instructions of the manufacturer. The samples were stored at – 20 °C until further utilisation.

4. Product quantification

Bioconversion of octane, styrene and cis- β -methyl styrene by a syringe pump and two-phase system. For product quantification the wild type enzyme and the best performing variants were purified as previously mentioned and the bioconversions were performed in triplicates. The following end concentrations were adjusted: 100 nM *MthUPO* variant (exception: bioconversion of styrene with 50 nM *MthUPO* variant), 1 mM H₂O₂ (a 2 mM stock solution was added by syringe pump with 200 µl/min), V_{total} = 400 µl, 100 mM KPi pH 7 and 200 µl of the substrate were added as organic layer. After one hour of H₂O₂ addition the solution was additionally stirred for 30 minutes. The organic layer was directly transferred for GC/MS analysis. The calibration curves were created under reaction conditions and were pictured in Fig. S5. For single GC-MS analysis the previously mentioned conditions were adjusted (Tab. S2). The samples were measured in scan mode and the corresponding *m/z* traces were filtered out for quantification. The calculated product concentration and turnover numbers (TONs) were listed in Tab. S4.

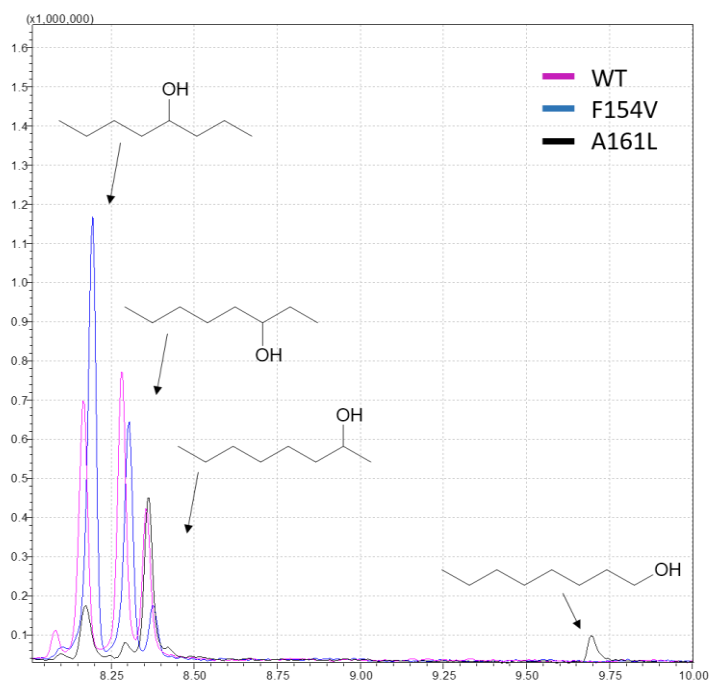
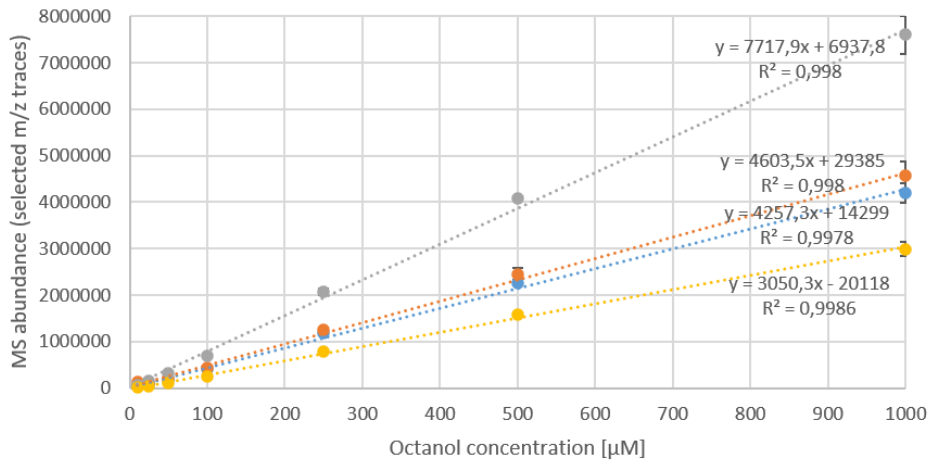


Fig. S4 GC-MS Chromatogram of the octane bioconversion with *MthUPO* wildtype, F154V and A161L.

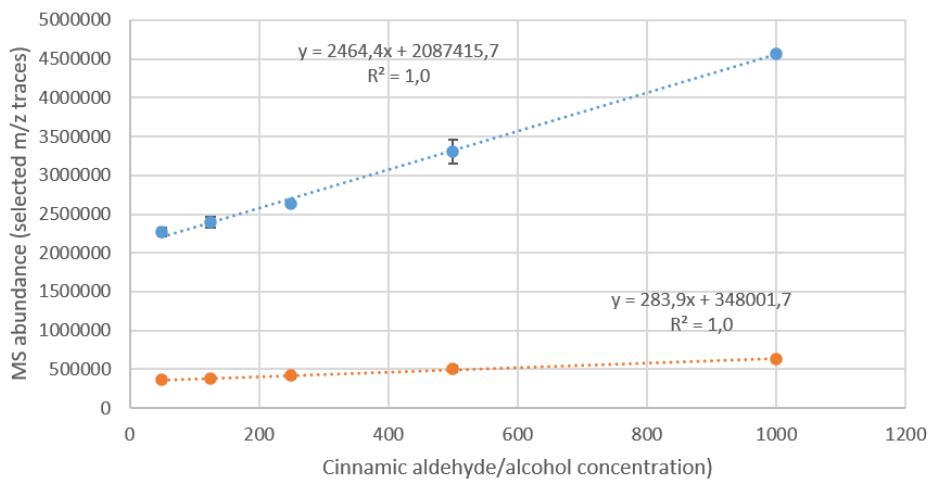
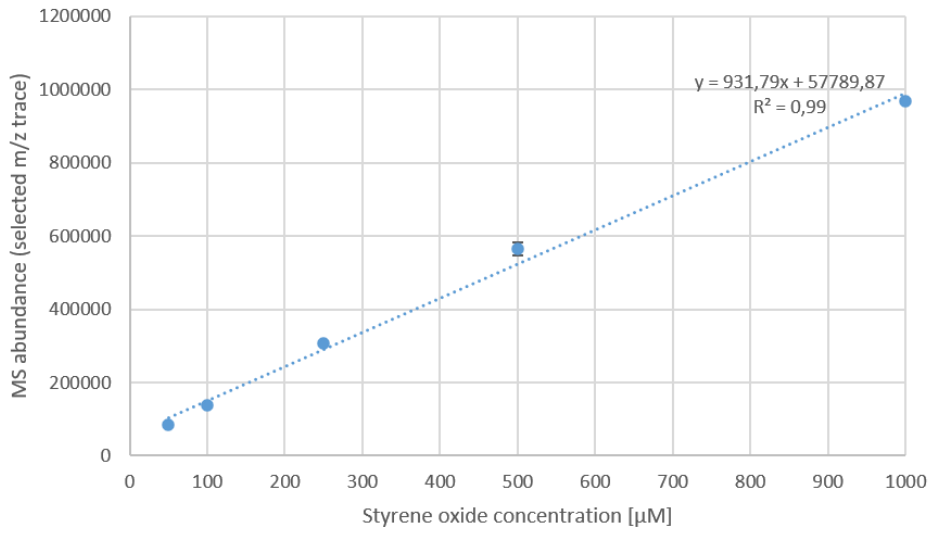
Tab. S4 Catalytic activity of purified *MthUPO* variants for the bioconversion of octane, styrene and *cis*- β -methyl styrene in a syringe pump and two-phase system.

Catalyst	Substrate \rightarrow Product	Concentration [μ M]	TON ^[a]
<i>MthUPO</i> WT	Octane		
	\rightarrow 1-octanol	-	-
	\rightarrow 2-octanol	20	200
	\rightarrow 3-octanol	29	290
	\rightarrow 4-octanol	20	200
<i>MthUPO</i> A161L	Octane		
	\rightarrow 1-octanol	8	80
	\rightarrow 2-octanol	21	210
	\rightarrow 3-octanol	-	-
	\rightarrow 4-octanol	20	20
<i>MthUPO</i> F154V	Octane		
	\rightarrow 1-octanol	-	-
	\rightarrow 2-octanol	5	50
	\rightarrow 3-octanol	20	200
	\rightarrow 4-octanol	36	360
<i>MthUPO</i> WT	Styrene		
	\rightarrow styrene oxide	111	1110
<i>MthUPO</i> A161L	Styrene		
	\rightarrow styrene oxide	503	5030
<i>MthUPO</i> WT	<i>cis</i> - β -methyl styrene		
	\rightarrow Cinnamic aldehyde	345	3450
	\rightarrow Cinnamic alcohol	199	1990
<i>MthUPO</i> A161L	<i>cis</i> - β -methyl styrene		
	\rightarrow Cinnamic aldehyde	329	3290
	\rightarrow Cinnamic alcohol	190	1900

TON = turnover number = product concentration/enzyme concentration, standard deviation < 11 %, [a] 100 nM *MthUPO* variant.



● 4-Octanol (m/z 69) ● 3-Octanol (m/z 59) ● 2-Octanol (m/z 45) ● 1-Octanol (m/z 41)



● Cinnamic aldehyde (m/z 131) ● Cinnamic alcohol (m/z 134)

Fig. S5 Calibration curves for the corresponding products from the two-phase systems.

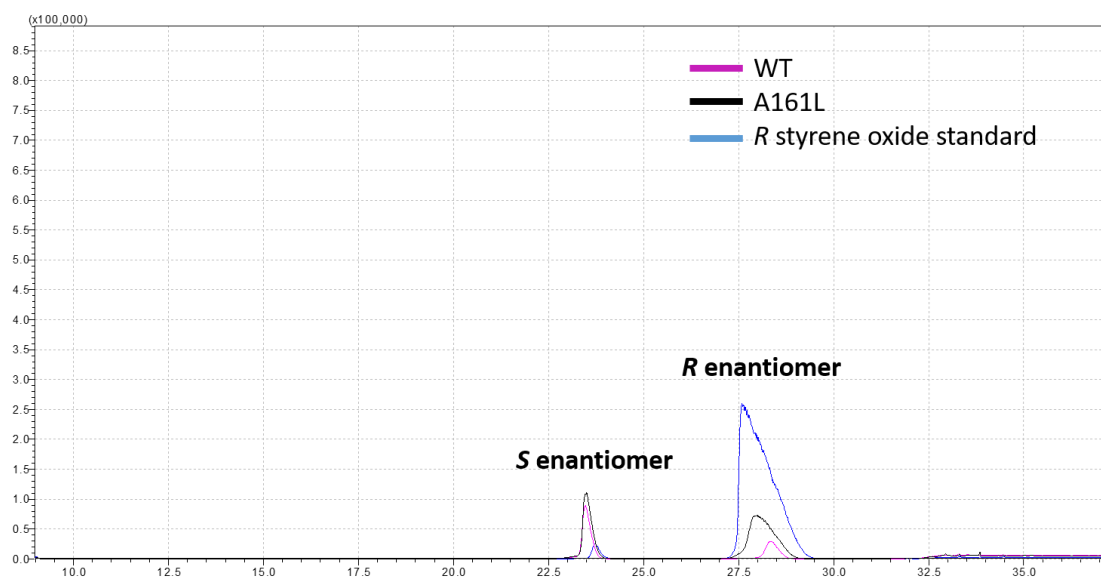


Fig. S6 GC-MS chromatogram of the chiral separation of styrene oxide in SIM mode (m/z : 119).

Bioconversion of cyclohexene, 1-methyl cyclohexene and α -methyl styrene by a syringe pump (without two-phase system). For product quantification the wild type enzyme and the best performing variants were purified as previously mentioned and the bioconversions were performed in triplicates. The following end concentrations were adjusted: 100 nM *MthUPO* variant, 1 mM H_2O_2 (a 2 mM stock solution was added by syringe pump with 200 μ l/min), $V_{total} = 400$ μ l, 100 mM KPi pH 7, 5 % (v/v) acetone and 1 mM of α -methyl styrene and 5 mM of cyclohexene/1-methylcyclohexene. After one hour of H_2O_2 addition the solution was additionally stirred for 30 minutes. Extraction was achieved by addition of 400 μ l EtOAc and 30 s of vortexing. The organic layer was transferred for GC/MS analysis. The calibration curves were created under reaction conditions and were pictured in Figure S9. The calibration for α -methyl styrene oxide was achieved by adaption of the calibration curve of styrene oxide. Therefore, the total ion current (TIC) was applied (Fig. S9). The compounds α -methyl styrene oxide were confirmed by literature comparison of the mass spectra⁴ and similarity library search by the GCMSolution software (Version 4.45, Shimadzu, Kyoto, JP) resulting the following mass spectrometric data: α -methyl styrene oxide (EI, 70 eV, m/z : 133, 103, 78, 51). The calibration of 1-methylcyclohexene oxide was achieved by adaption of the calibration curve of cyclohexene oxide by applying the TIC (Fig. S9). The literature comparison⁵ as well as the similarity library search by the GCMSolution software (Version 4.45, Shimadzu, Kyoto, JP) confirmed 1-methylcyclohexene oxide as compound with the following mass spectrometric data: EI, 70 eV, m/z : 112, 111, 97, 83, 69, 55, 43. In addition to 1-methylcyclohexene oxide, unknown hydroxylation products were detected as shown in Fig. S8. We were not able to identify the corresponding product based on literature comparison. For single GC-MS analysis the previously mentioned conditions were adjusted (Tab. S2). For cyclohexene oxide the samples were measured in scan mode and the corresponding m/z traces were filtered out for quantification.

Tab. S5 Catalytic activity of purified *MthUPO* variants for the bioconversion of cyclohexene and α -methyl styrene with the help of a syringe pump setup.

Catalyst	Substrate \rightarrow Product	Concentration [μ M]	TON ^[a]
<i>MthUPO</i> WT	Cyclohexene \rightarrow cyclohexene oxide	404	4040
<i>MthUPO</i> A161L	Cyclohexene \rightarrow cyclohexene oxide	438	4380
<i>MthUPO</i> L60A	Cyclohexene \rightarrow cyclohexene oxide	116	1160
<i>MthUPO</i> WT	α -methyl styrene \rightarrow α -methyl styrene oxide	184	1840
<i>MthUPO</i> A161L	α -methyl styrene \rightarrow α -methyl styrene oxide	233	2330

TON = turnover number = product concentration/enzyme concentration, standard deviation < 15 %, [a] 100 nM *MthUPO* variant.

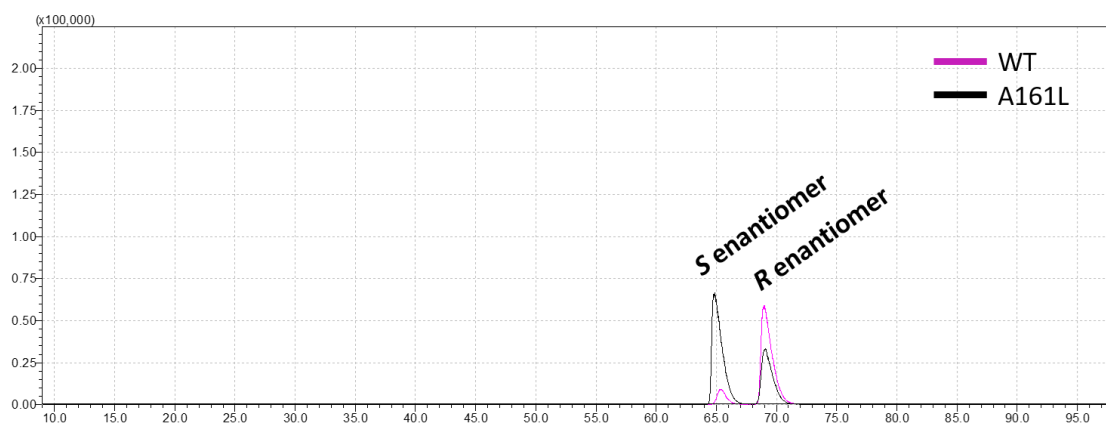


Fig. S7 GC-MS chromatogram of the chiral separation of α -methylstyrene oxide in SIM mode (m/z : 133).

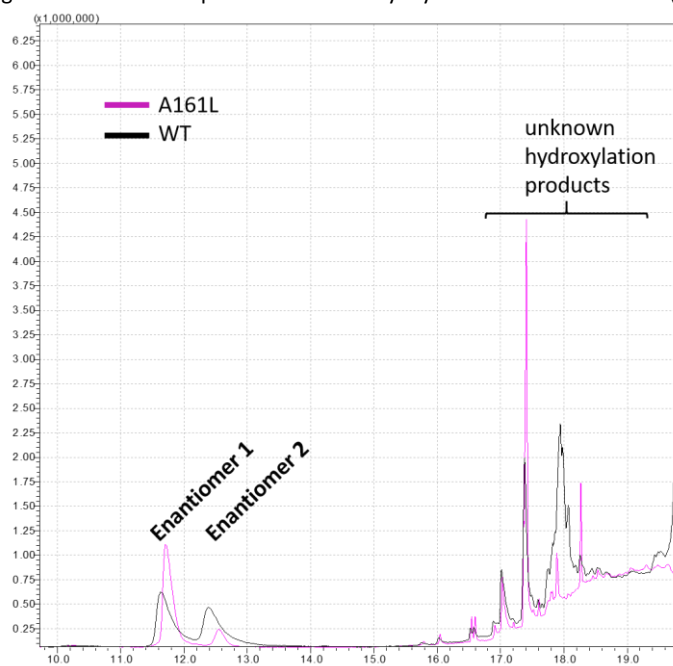


Fig. S8 GC-MS chromatogram of the chiral separation of 1-methylcyclohexene oxide in TIC mode.

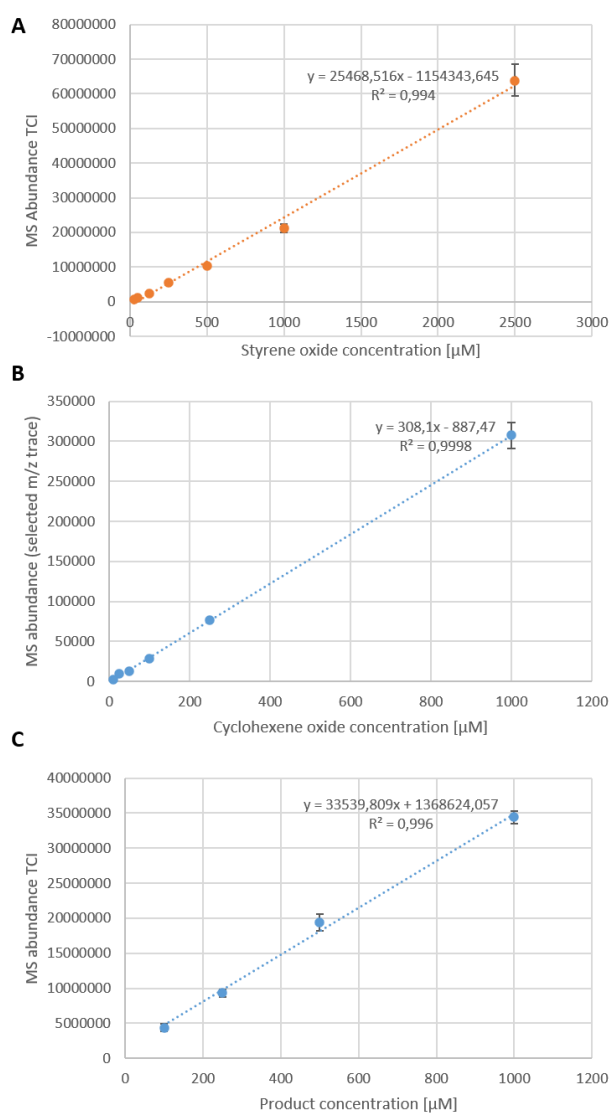


Fig. S9 Calibration curves for the corresponding products from a one phase system: A) calibration of styrene oxide in total ion current (TCI) mode for quantification of α -methylstyrene, B) calibration curve of cyclohexene oxide and C) calibration of cyclohexene oxide in TCI mode for quantification of 1-methylcyclohexene oxide.

Tab. S6 Overview of the chiral measured substrates with the corresponding *MthUPO* variants.

Catalyst	Substrate → Product	% ee (Enantiomer)
<i>MthUPO</i> WT	1-methylcyclohexene → 1-methylcyclohexene oxide	17 (unknown enantiomer)
<i>MthUPO</i> A161L	1-methylcyclohexene → 1-methylcyclohexene oxide	75 (unknown enantiomer)
<i>MthUPO</i> L60A	1-methylcyclohexene → 1-methylcyclohexene oxide	6 (unknown enantiomer, TON: 1070)
<i>MthUPO</i> WT	styrene → styrene oxide	32 (<i>R</i>)
<i>MthUPO</i> A161L	styrene → styrene oxide	28 (<i>S</i>)
<i>MthUPO</i> WT	α -methyl styrene → α -methyl styrene oxide	77 (<i>R</i>)
<i>MthUPO</i> A161L	α -methyl styrene → α -methyl styrene oxide	29 (<i>S</i>)

Standard deviation < 8 %, reaction conditions were mentioned above.

Negative controls for the bioconversion of styrene. The bioconversion samples of styrene had to be injected into the GC-MS at lowered injection temperatures (100/180 °C) due to the decomposition of styrene oxide at high temperature in the GC liner (Fig. S10). Beside the increase product formation of styrene oxide with the *MthUPO* variant A161L (compared to the wild type), a second product was detected within the GC-MS analysis which was identified as phenylacetaldehyde. In order to confirm the enzymatical product formation of the aldehyde negative controls were performed: I) 100 nM heat inactivated *MthUPO* A161L (90 °C for 1 h) was utilised under the previously mentioned reaction conditions in a two-phase system with a syringe pump setup yielding to no detection of styrene oxide nor the phenylacetaldehyde (Fig. S11, orange), II) no enzyme was utilised to check the background activity of this setup under the previously mentioned reaction conditions in a two-phase system with a syringe pump setup yielding to no product formation (Fig. S11, blue), III) no enzyme was utilised in presence of 1 mM styrene oxide to determine the decomposition of the product under reaction conditions in a two-phase system with a syringe pump setup which yielded to no detection of the aldehyde (Fig. S11, grey) confirming the enzymatically catalysed formation of the aldehyde.

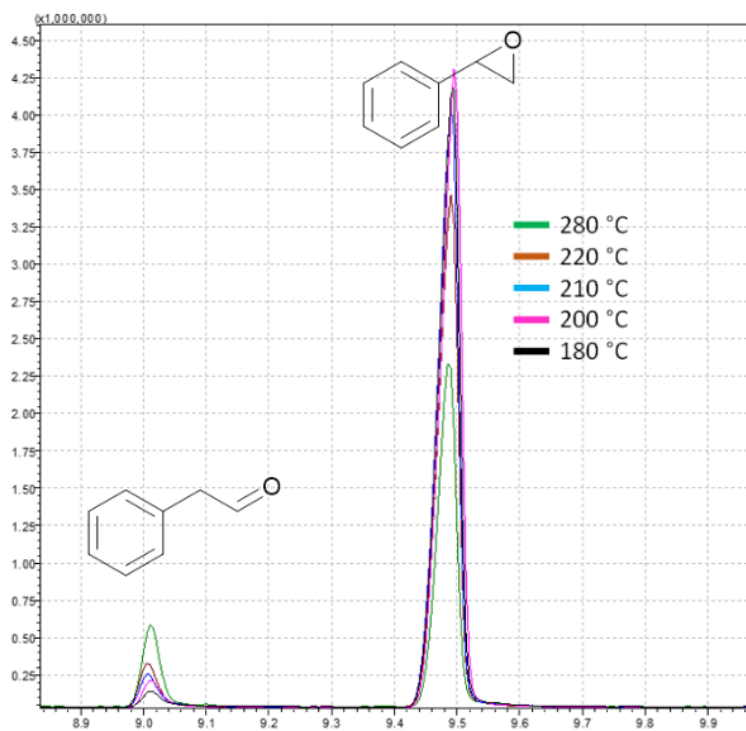


Fig. S10 Decomposition of styrene oxide to phenylacetaldehyde under altered GC injection temperatures.

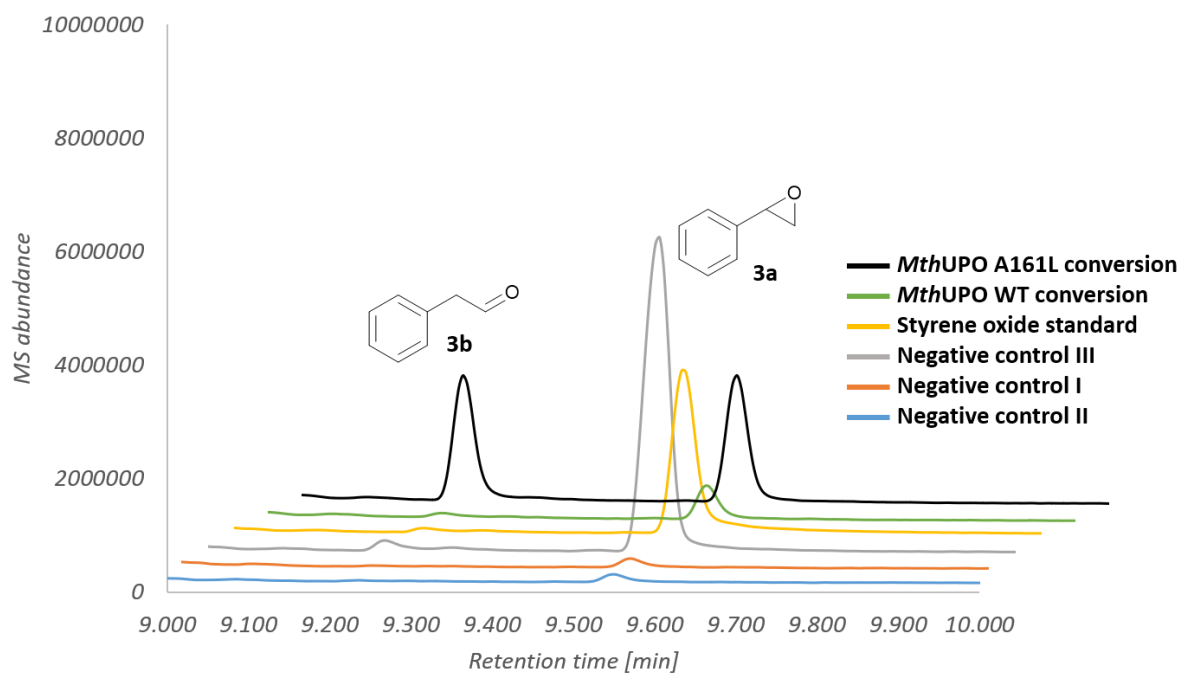


Fig. S11 GC-MS chromatograms of the *MthUPO* catalysed bioconversions of styrene, styrene oxide as injected standard and negative controls.

5. Computational details

Quantum Mechanics (QM) calculations. A truncated computational model has been used to model the C-H activation and epoxidation of different studied substrates. The truncated model used [Fe=O(Por)(SCH₃)(substrate)] includes: the active Fe-oxo species (Fe=O), the porphyrin pyrrole core (Por), a methyl thiolate group (-SCH₃) to mimic Cysteine axial ligand, and cyclohexane, cyclohexene, or octane as substrates. Density Functional Theory (DFT) calculations were carried out using Gaussian09 software package.⁶ Geometry optimizations and frequency calculations were performed using (U)B3LYP⁷ functional with 6-31G(d) basis set on all atoms except for Fe, where SDD basis set and related SDD pseudopotential were employed. An *ultrafine* integration grid was used. The optimized geometries were verified as minima by a vibrational frequency analysis and transition states geometries have a single imaginary frequency consistent with the reaction coordinate. Enthalpies and entropies were calculated for 1 atm and 298.15 K. A correction to the harmonic oscillator approximation, as discussed by Truhlar and co-workers, was also applied to the enthalpy calculations by raising all frequencies below 100 cm⁻¹ to 100 cm⁻¹⁸ using Goodvibes v.1.0.1 python script.⁹ Single point energy calculations were performed using the functional (U)B3LYP with the Def2TZVP basis set on all atoms, and within the CPCM polarizable conductor model (dichloromethane, $\epsilon = 8.9$)¹⁰ to have an estimation of the dielectric permittivity in the enzyme active site.¹¹ Empirical Grimme D3 dispersion corrections with Becke-Johnson (D3BJ) damping are also included in single point calculations.¹² All structures have a total neutral charge and calculations were performed with doublet (d) or quartet (q) multiplicities consistent with the expected electronic states of the heme cofactor.

Homology model and Molecular Dynamics (MD) simulations. Homology model for *Mth*UPO structure (283 AA) obtained from our previous work has been used as starting point.¹³ Molecular Dynamics (MD) simulations in explicit water were performed using the AMBER18 package.¹⁴ Parameters for the octane and cyclohexene substrates were generated within the antechamber¹⁵ module in AMBER18 package using the general AMBER force field (gaff)¹⁶, with partial charges set to fit the electrostatic potential generated at the B3LYP/6-31G(d) level by the RESP model.¹⁷ The charges were calculated according to the Merz–Singh–Kollman scheme¹⁸ using the Gaussian 09 package. Parameters for the heme compound I (Cpd I) and the axial Cys were taken from reference.¹⁹ The protein was solvated in a pre-equilibrated cubic box with a 12-Å buffer of TIP3P²⁰ water molecules using the AMBER18 leap module, resulting in the addition of ~17,500 solvent molecules. The systems were neutralized by addition of explicit counterions (Na⁺ and Cl⁻). All subsequent calculations were done using the AMBER force field 14 Stony Brook (ff14SB).²¹ A two-stage geometry optimization approach was performed. The first stage minimizes the positions of solvent molecules and ions imposing positional restraints on solute by a harmonic potential with a force constant of 500 kcal mol⁻¹ Å⁻², and the second stage is an unrestrained minimization of all the atoms in the simulation cell. The systems were gently heated using six 50 ps steps, incrementing the temperature by 50 K for each step (0–300 K) under constant-volume and periodic-boundary conditions. Water molecules were treated with the SHAKE algorithm such that the angle between the hydrogen atoms was kept fixed. Long-range electrostatic effects were modelled using the particle-mesh-Ewald method.²² An 8 Å cutoff was applied to Lennard–Jones and electrostatic interactions. Harmonic restraints of 30 kcal·mol⁻¹ were applied to the solute, and the Langevin equilibration scheme was used to control and equalize the temperature. The time step was kept at 1 fs during the heating stages, allowing potential inhomogeneities to self-adjust. Each system was then equilibrated for 2 ns with a 2 fs time step at a constant pressure of 1 atm and temperature of 300 K without restraints. Once the systems were equilibrated in the NPT ensemble, production trajectories were then run under the NVT ensemble and periodic-boundary conditions. In particular, a total of 3000 ns were accumulated for L60A variant from 3 independent replicas (3x 1000 ns); and 1500 ns

were accumulated for A161L variant from 3 independent replicas (500 ns each). An extensive conformational sampling based on longer and additional MD replicas has been carried out to refine the initial homology model. Trajectories were processed and analyzed using the cptraj²³ module from Amber tools utilities.

Docking and protocol used for substrate bound MD simulations. Docking calculations were performed using AutoDock Vina.²⁴ The most populated clusters (based on backbone clustering analysis) obtained from MD simulations carried out in the absence of substrate were used, and docking predictions were then utilized as starting points for substrate-bound MD simulations without any external restraints. Same protocol for MD simulations described above has been employed, accumulating a total of 300 ns of production trajectories from 3 independent replicas for all studied substrates. Trajectories were processed and analyzed using the cptraj module from Amber tools utilities.

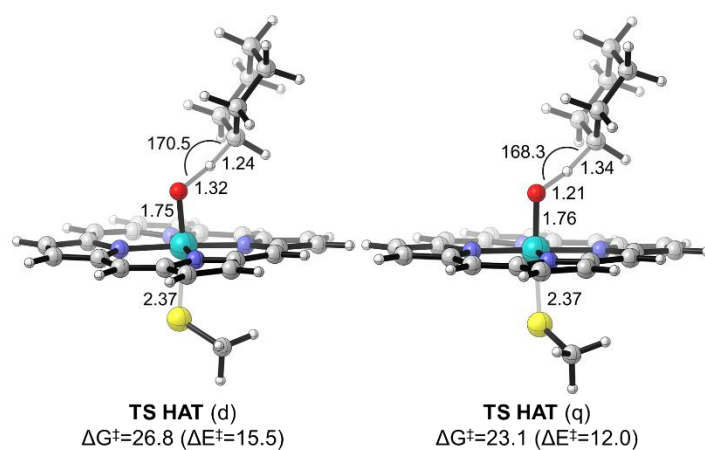


Figure S12. DFT model calculations exploring the hydroxylation of cyclohexane. Optimized structures for the Hydrogen Atom Transfer Transition State (HAT TS) involved in cyclohexane hydroxylation and their computed relative energies in terms of electronic energy (ΔE^\ddagger) and quasi-harmonic corrected Gibbs energy (ΔG^\ddagger). Energy values were obtained at the (U)B3LYP-D3BJ/Def2TZVP/PCM(dichloromethane)//(U)B3LYP/6-31G(d)+SDD(Fe)/PCM (dichloromethane) level. Energies are referred considering reactants structures as zero. All energies are given in kcal·mol⁻¹. Distances and angles are given in Angstrom (Å) or degrees (°), respectively.

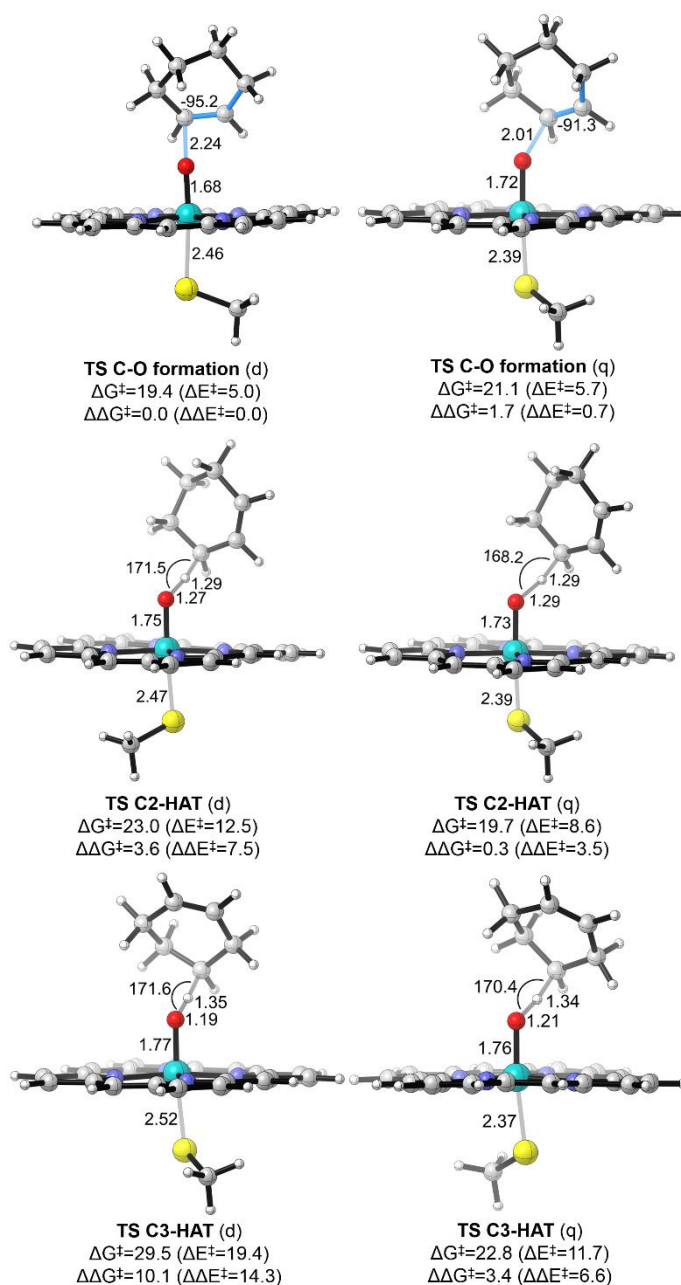
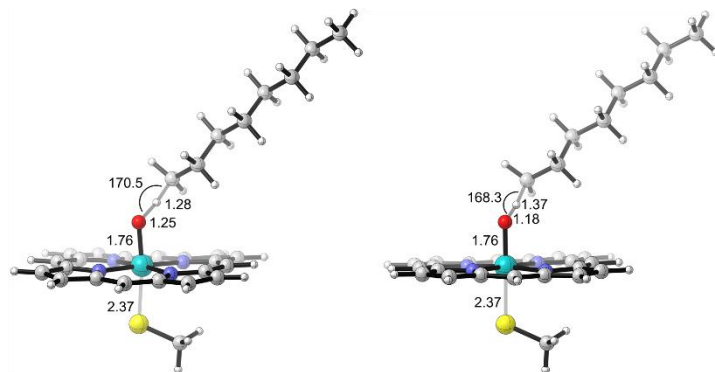
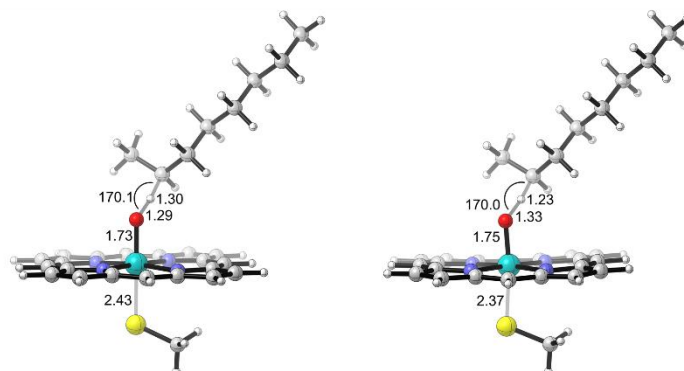


Figure S13. DFT model calculations exploring the hydroxylation and epoxidation of cyclohexene. Optimized structures for the different Hydrogen Atom Transfer Transition States (HAT TS) involved in cyclohexane hydroxylation and TS C-O formation involved in cyclohexene epoxidation and their computed relative energies in terms of electronic energy (ΔE^\ddagger) and quasi-harmonic corrected Gibbs energy (ΔG^\ddagger). Energy values were obtained at the (U)B3LYP-D3BJ/Def2TZVP/PCM(dichloromethane)//(U)B3LYP/6-31G(d)+SDD(Fe)/PCM(dichloromethane) level. Energies are referred considering reactants structures as zero and relative differences between TS are also reported. All energies are given in kcal·mol⁻¹. Distances, angles, and dihedrals are given in Angstrom (Å) or degrees (°), respectively.



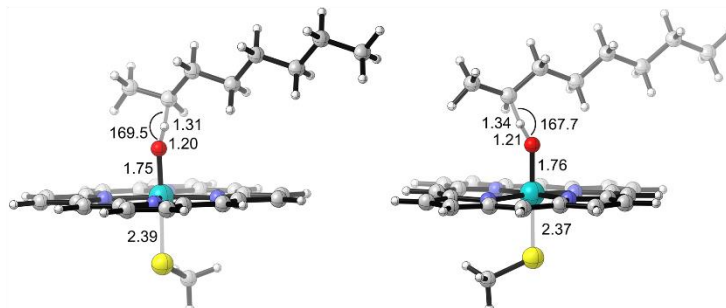
TS C1-HAT (d)
 $\Delta G^\ddagger=33.4$ ($\Delta E^\ddagger=20.1$)
 $\Delta\Delta G^\ddagger=11.6$ ($\Delta\Delta E^\ddagger=12.0$)

TS C1-HAT (q)
 $\Delta G^\ddagger=28.5$ ($\Delta E^\ddagger=15.4$)
 $\Delta\Delta G^\ddagger=6.7$ ($\Delta\Delta E^\ddagger=7.3$)



TS C2-HAT (d)
 (conformation 1)
 $\Delta G^\ddagger=29.5$ ($\Delta E^\ddagger=16.0$)
 $\Delta\Delta G^\ddagger=7.7$ ($\Delta\Delta E^\ddagger=7.9$)

TS C2-HAT (q)
 (conformation 1)
 $\Delta G^\ddagger=26.0$ ($\Delta E^\ddagger=13.1$)
 $\Delta\Delta G^\ddagger=4.1$ ($\Delta\Delta E^\ddagger=5.0$)



TS C2-HAT (d)
 (conformation 2)
 $\Delta G^\ddagger=27.4$ ($\Delta E^\ddagger=13.6$)
 $\Delta\Delta G^\ddagger=5.5$ ($\Delta\Delta E^\ddagger=5.5$)

TS C2-HAT (q)
 (conformation 2)
 $\Delta G^\ddagger=23.7$ ($\Delta E^\ddagger=10.3$)
 $\Delta\Delta G^\ddagger=1.8$ ($\Delta\Delta E^\ddagger=2.2$)

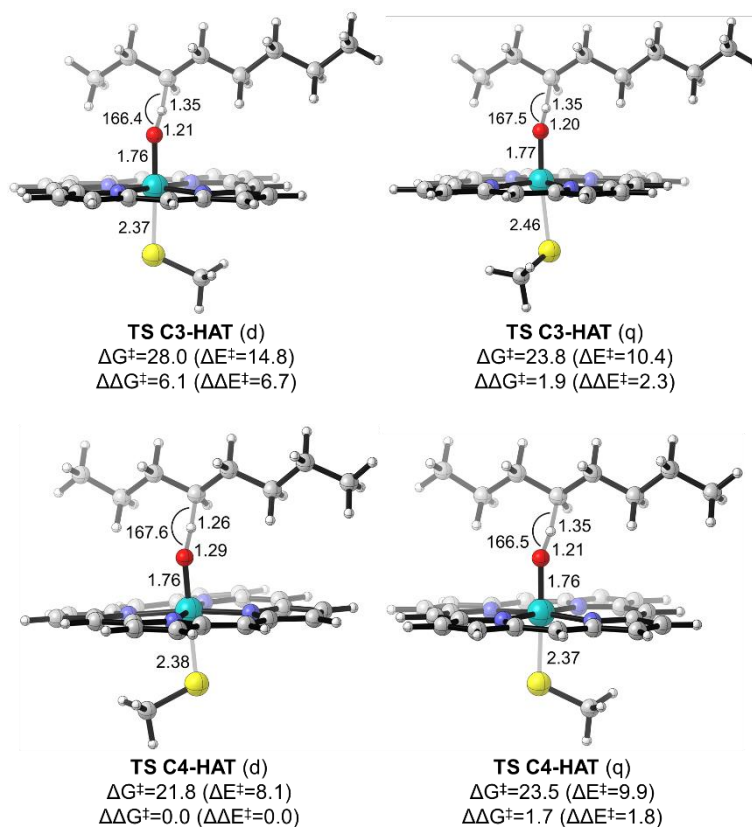


Figure S14. DFT model calculations exploring the hydroxylation of octane. Optimized structures for the Hydrogen Atom Transfer Transition State (HAT TS) involved in octane hydroxylation in different positions and their computed relative energies in terms of electronic energy (ΔE^\ddagger) and quasi-harmonic corrected Gibbs energy (ΔG^\ddagger). Energy values were obtained at the (U)B3LYP-D3BJ/Def2TZVP/PCM(dichloromethane)//(U)B3LYP/6-31G(d)+SDD (Fe)/PCM(dichloromethane) level. Energies are referred considering reactants structures as zero. All energies are given in $\text{kcal}\cdot\text{mol}^{-1}$. Distances and angles are given in Angstrom (\AA) or degrees ($^\circ$), respectively.

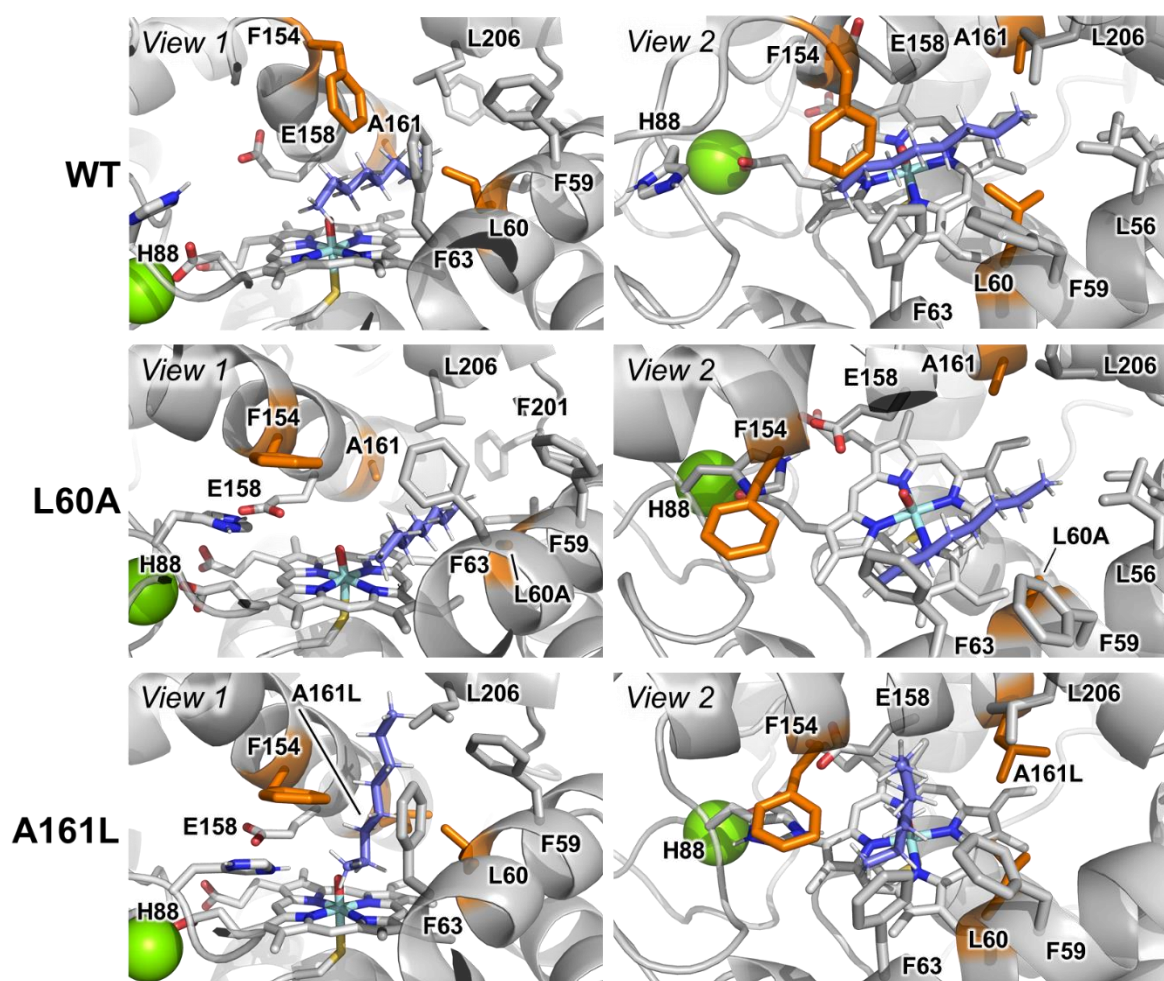
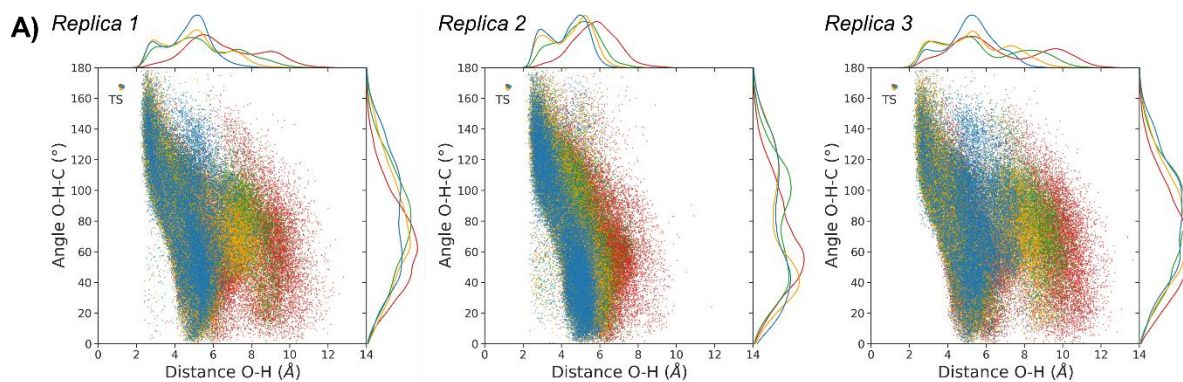
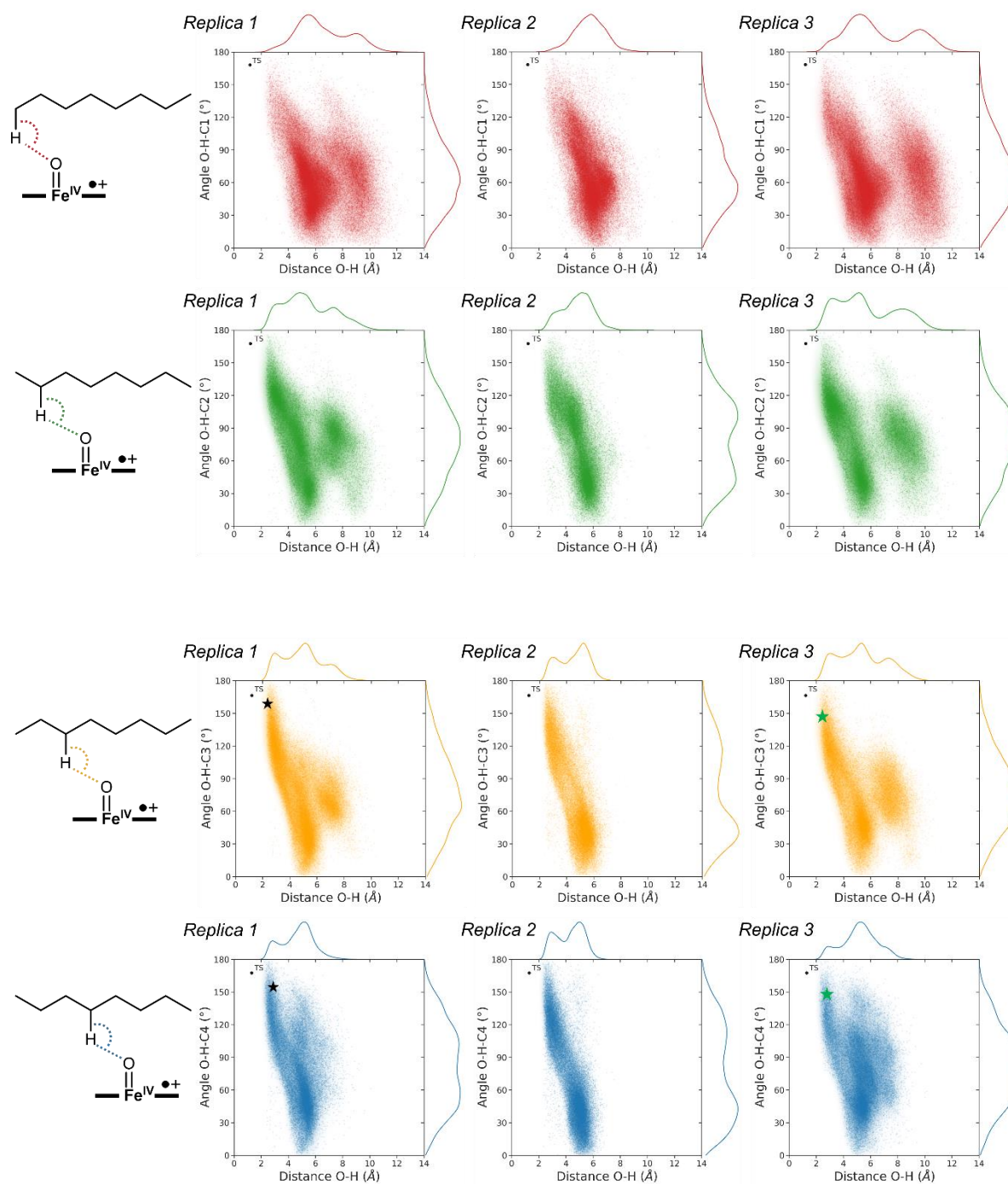


Figure S15. Exploration of octane catalytically relevant binding poses in WT, L60A and A161L variants as observed from MD simulations (see **Figure S16, S17, and S18**). Mutated positions are highlighted in orange. The residues shown in sticks format are found to establish important hydrophobic interactions with octane (except the catalytic E158 and H88 residues).

Octane explores different preferential near attack conformations (NACs) in each studied variant due to the new introduced mutations. L60A increases the active site cavity allowing octane to explore less constrained conformations, being placed further from the reactive Cpd I as compared to the WT. A161L prevents octane to bind deeper in the active site, and it explores a new binding mode vertical to the heme cofactor occupying part of the substrate entrance channel. In this new binding mode terminal C-H positions are preferentially exposed to Cpd I to react.



B)



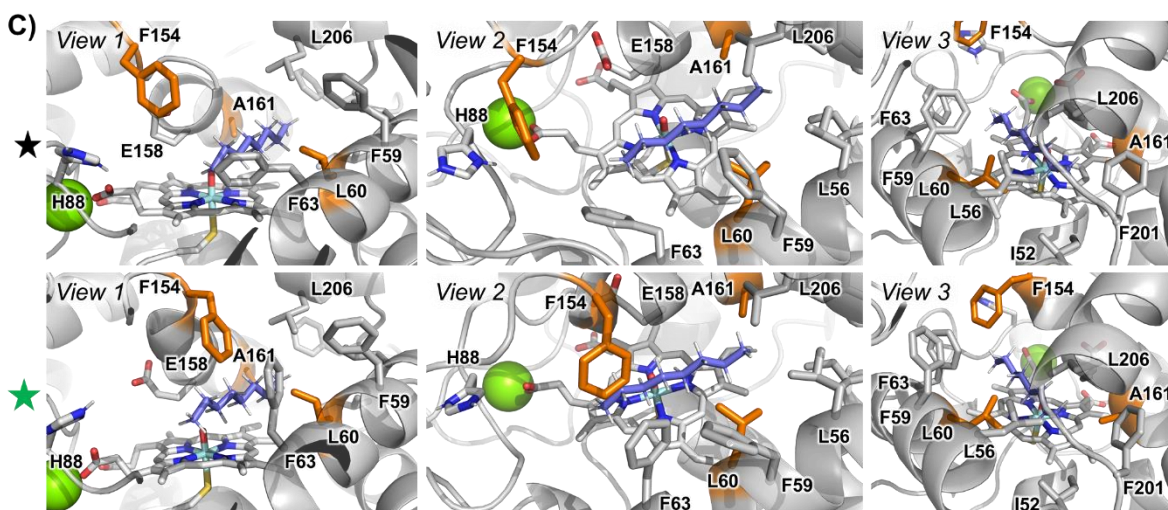
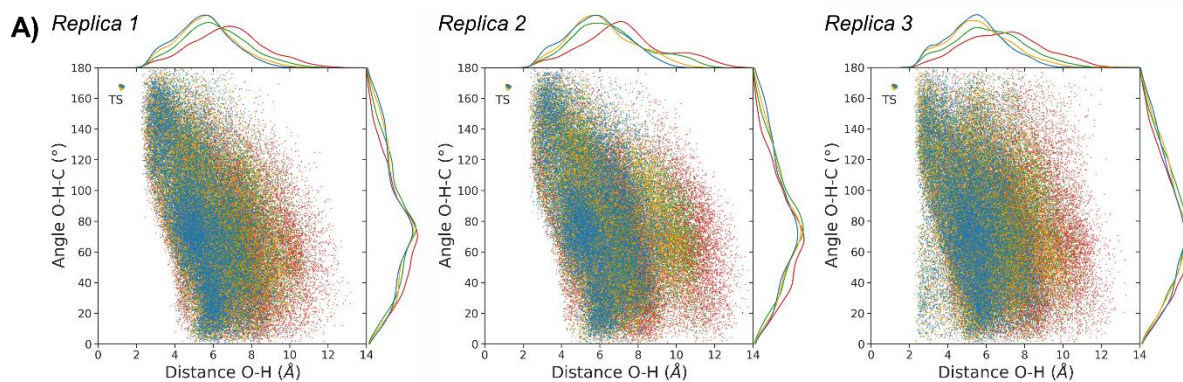
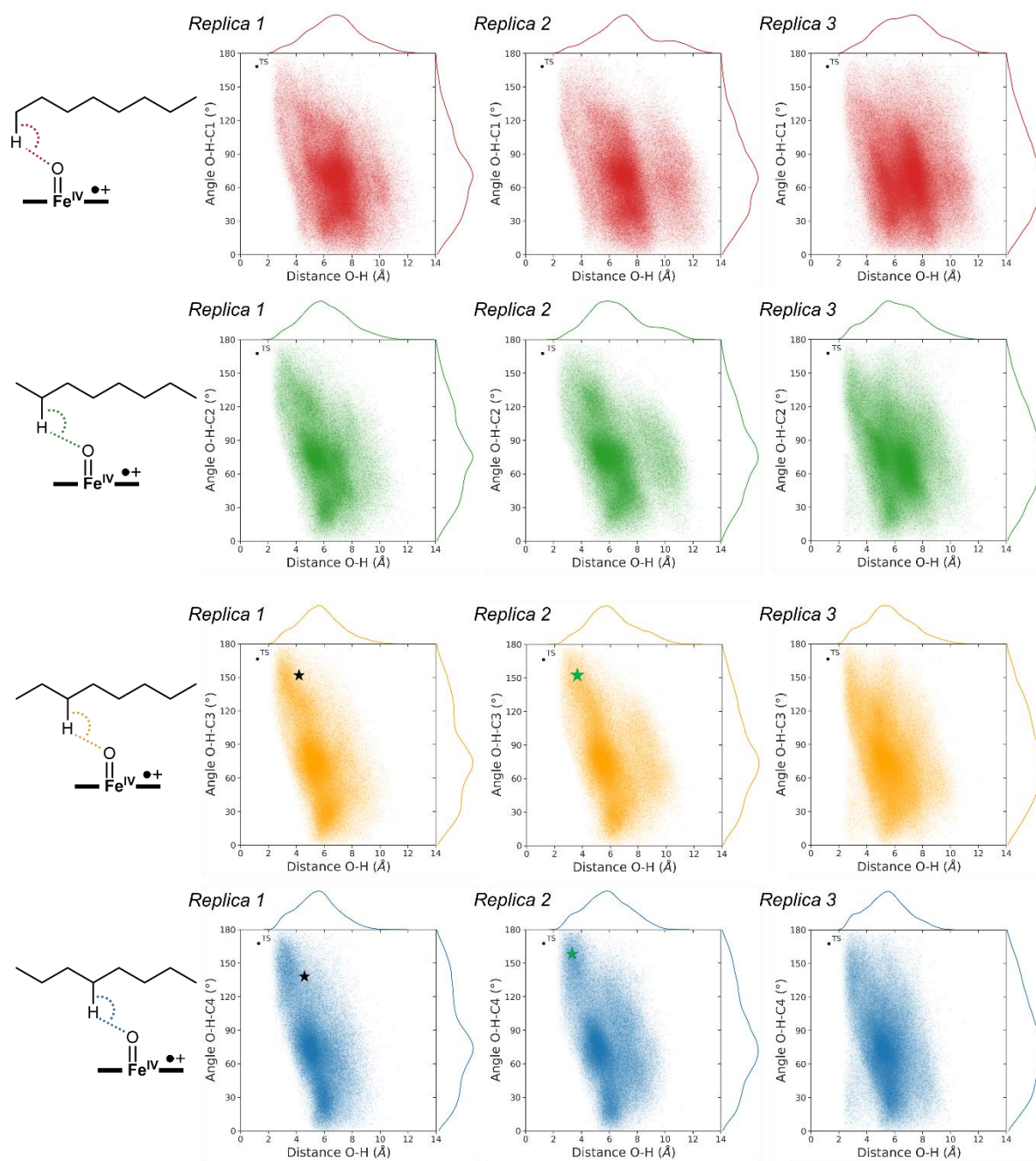


Figure S16. Analysis of octane binding poses in WT MthUPO through MD simulations. Fe=O – H(-C-octane) distance and angle of attack (O-H-C) are used as geometric parameters to characterize near attack conformations for effective C-H octane hydroxylation utilizing heat map representations. **A)** Overlay of heat maps for near attack conformations explored by each non-equivalent C-H position (C1 red, C2 green, C3 yellow, C4 blue) obtained from 3 independent MD simulations. **B)** Independent heat maps for near attack conformations explored by each non-equivalent C-H position (C1 red, C2 green, C3 yellow, C4 blue) obtained from 3 independent MD simulations. Ideal geometric parameters for C-H abstraction obtained from DFT Transition State (TS) optimizations are shown. **C)** Representative structures from MD trajectories (highlighted with an “star” symbol) that describe reactive near attack conformations explored during MDs are shown. Distances and angles are given in angstroms (Å) and degrees (°), respectively.

Angle vs. distance heat maps indicate that octane can explore catalytically competent poses in which C4, C3 and C2 C–H bonds can explore near attack conformations (geometric parameters close to the TS ideal ones) that are expected to lead to 4-octanol and 3-octanol 2-octanol products. On the other hand, C1 position stays far from the Cpd I active species. See **Figure S15** for a comparison between octane binding poses in different studied MthUPO variants.



B)



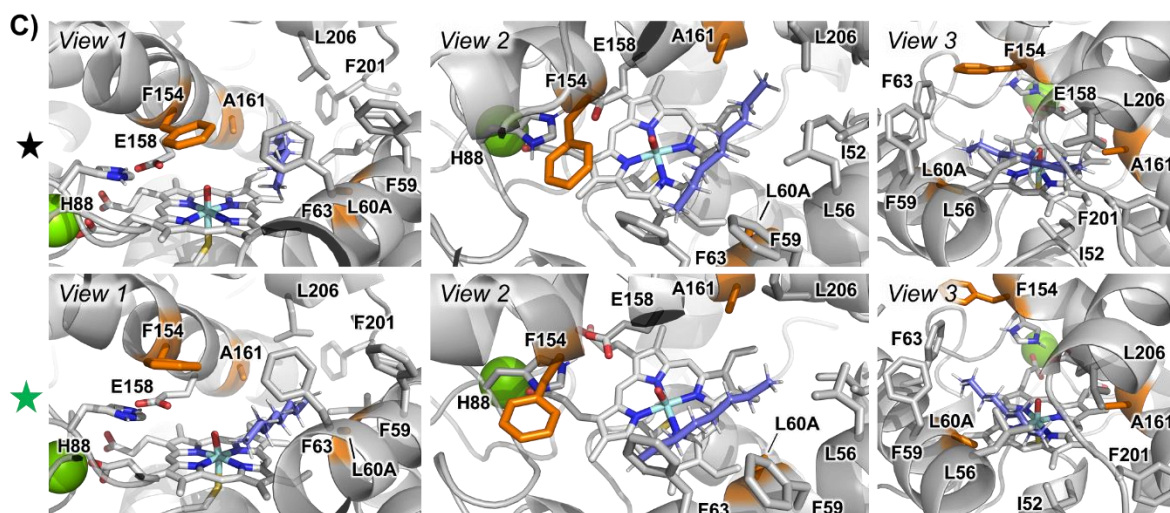
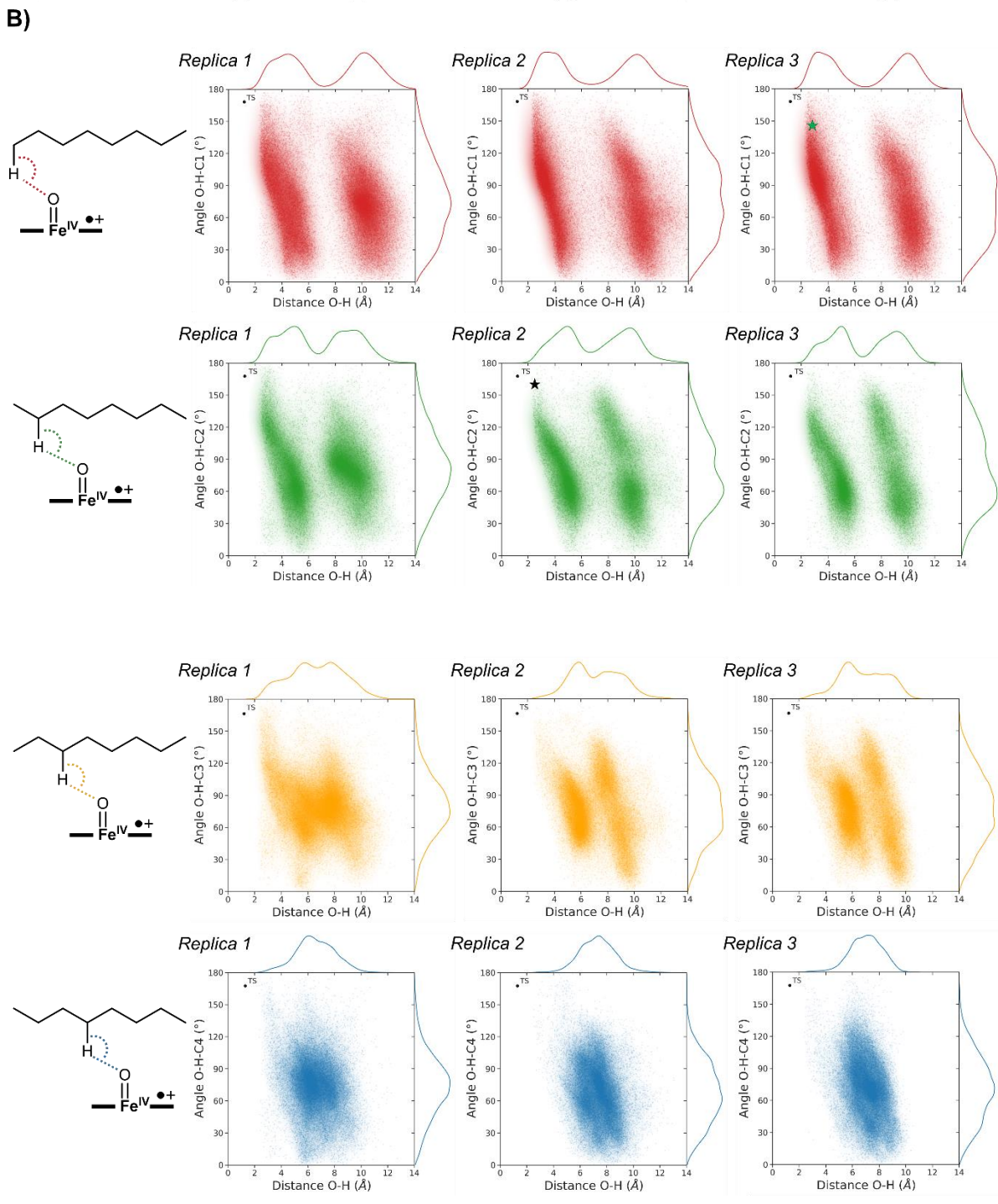
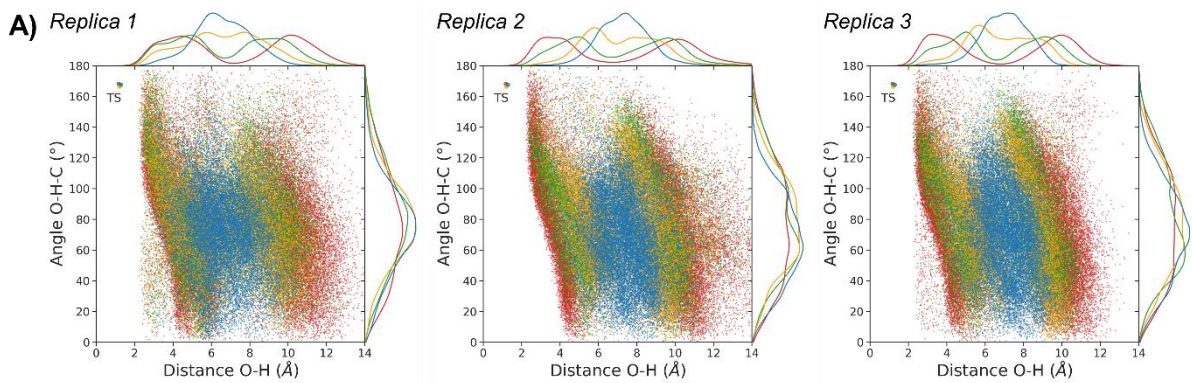


Figure S17. Analysis of octane binding poses in L60A MthUPO through MD simulations. $\text{Fe}=\text{O} - \text{H}(\text{-C-octane})$ distance and angle of attack (O-H-C) are used as geometric parameters to characterize near attack conformations for effective C-H octane hydroxylation utilizing heat map representations. **A)** Overlay of heat maps for near attack conformations explored by each non-equivalent C-H position (C1 red, C2 green, C3 yellow, C4 blue) obtained from 3 independent MD simulations. **B)** Independent heat maps for near attack conformations explored by each non-equivalent C-H position (C1 red, C2 green, C3 yellow, C4 blue) obtained from 3 independent MD simulations. Ideal geometric parameters for C-H abstraction obtained from DFT Transition State (TS) optimizations are shown. **C)** Representative structures from MD trajectories (highlighted with an “star” symbol) that describe reactive near attack conformations explored during MDs are shown. Distances and angles are given in angstroms (\AA) and degrees ($^\circ$), respectively.

Angle vs. distance heat maps show that octane binding in L60A active site is more flexible as compared to WT, thus leading to the exploration of less competent near attack conformations than in WT (i.e. decreased activity).

MD simulation analysis also indicate that L60A variant would perform regioselective octane hydroxylation in a similar manner than the WT enzyme (**Figure S16**). See **Figure S15** for a comparison between octane binding poses in different studied MthUPO variants.



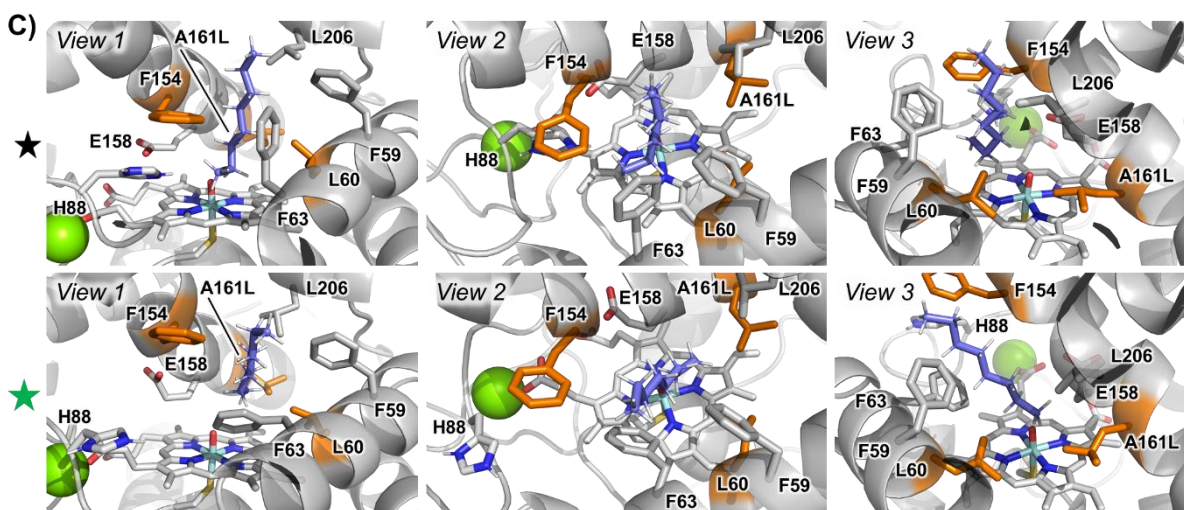


Figure S18. Analysis of octane binding poses in A161L MthUPO through MD simulations. Fe=O – H(-C-octane) distance and angle of attack (O-H-C) are used as geometric parameters to characterize near attack conformations for effective C-H octane hydroxylation utilizing heat map representations. **A)** Overlay of heat maps for near attack conformations explored by each non-equivalent C-H position (C1 red, C2 green, C3 yellow, C4 blue) obtained from 3 independent MD simulations. **B)** Independent heat maps for near attack conformations explored by each non-equivalent C-H position (C1 red, C2 green, C3 yellow, C4 blue) obtained from 3 independent MD simulations. Ideal geometric parameters for C-H abstraction obtained from DFT Transition State (TS) optimizations are shown. **C)** Representative structures from MD trajectories (highlighted with an “star” symbol) that describe reactive near attack conformations explored during MDs are shown. Distances and angles are given in angstroms (Å) and degrees (°), respectively.

Angle vs. distance heat maps indicate that octane can explore catalytically competent poses in which C1 and C2 C–H bonds can explore near attack conformations (geometric parameters close to the TS ideal ones) that are expected to lead to 1-octanol and 2-octanol products. On the other hand, C3 and C4 positions are found to be further from the Cpd I active species. This is due to the preferential binding pose that octane explores because of the presence of A161L mutation. See **Figure S15** for a comparison between preferential octane binding poses in the different studied *MthUPO* variants.

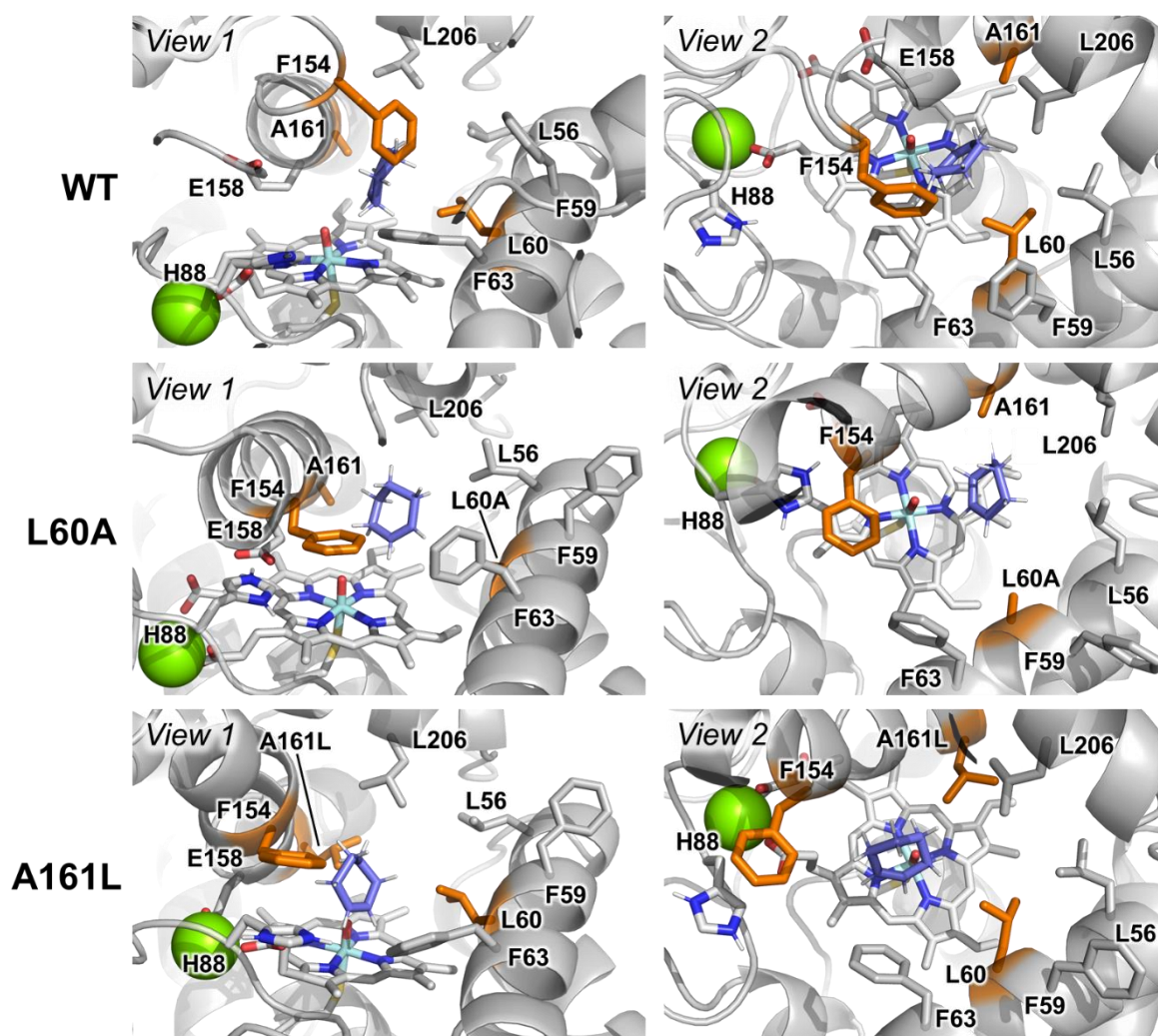
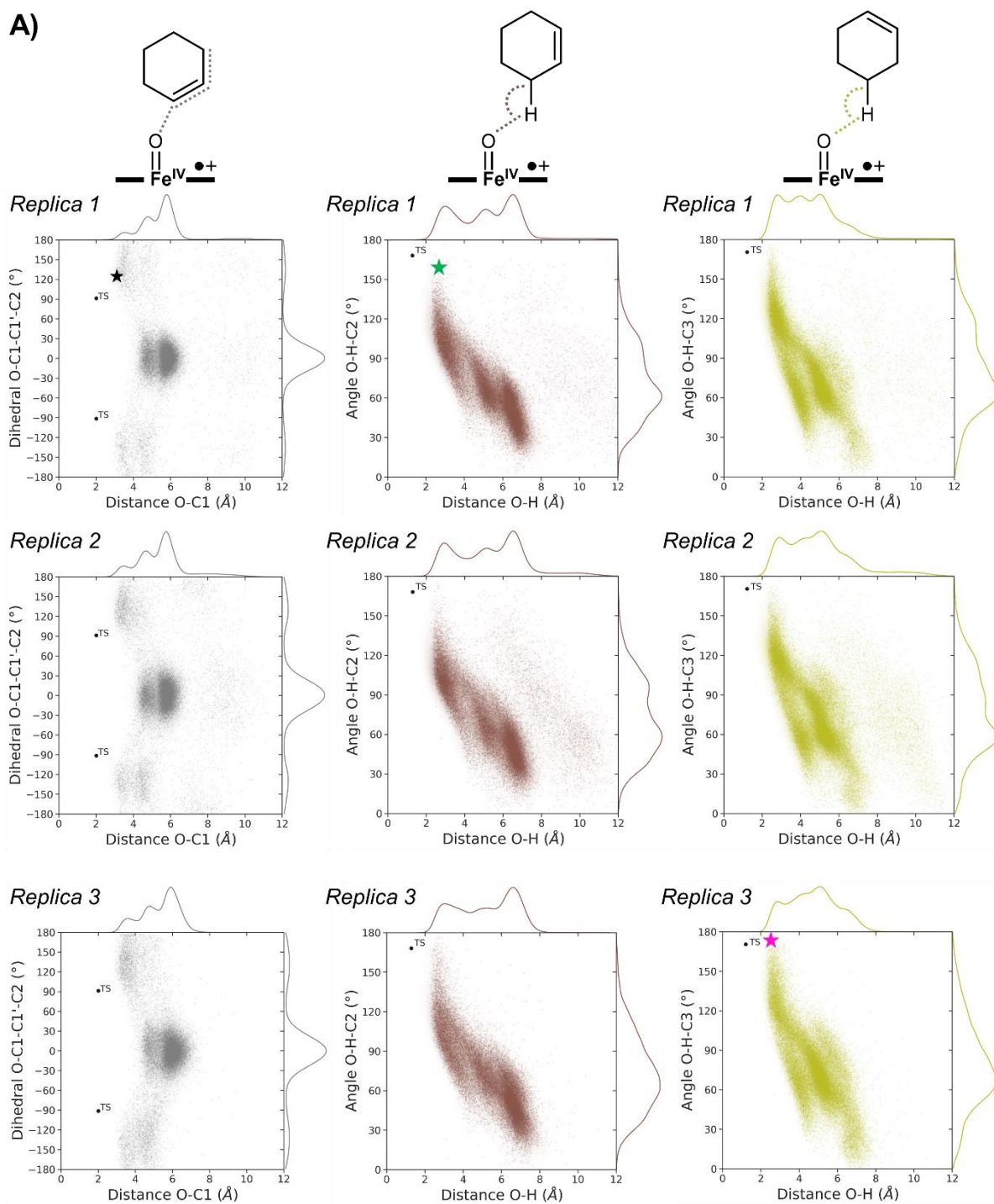


Figure S19. Exploration of cyclohexene catalytically relevant binding poses in WT, L60A, and A161L variants as observed from MD simulations (see **Figure S20, S21, and S22**). Mutated positions are highlighted in orange. The residues shown in sticks format are found to establish important hydrophobic interactions with cyclohexene (except the catalytic E158 and H88 residues).

Cyclohexene explores similar binding poses in WT and L60A variant. L60A increases the active site cavity, allowing cyclohexene to have a more flexible binding pose. A161L mutation prevents cyclohexene to occupy the original binding position, being placed next to the entrance channel closer to F154 and F63 residues.

A)

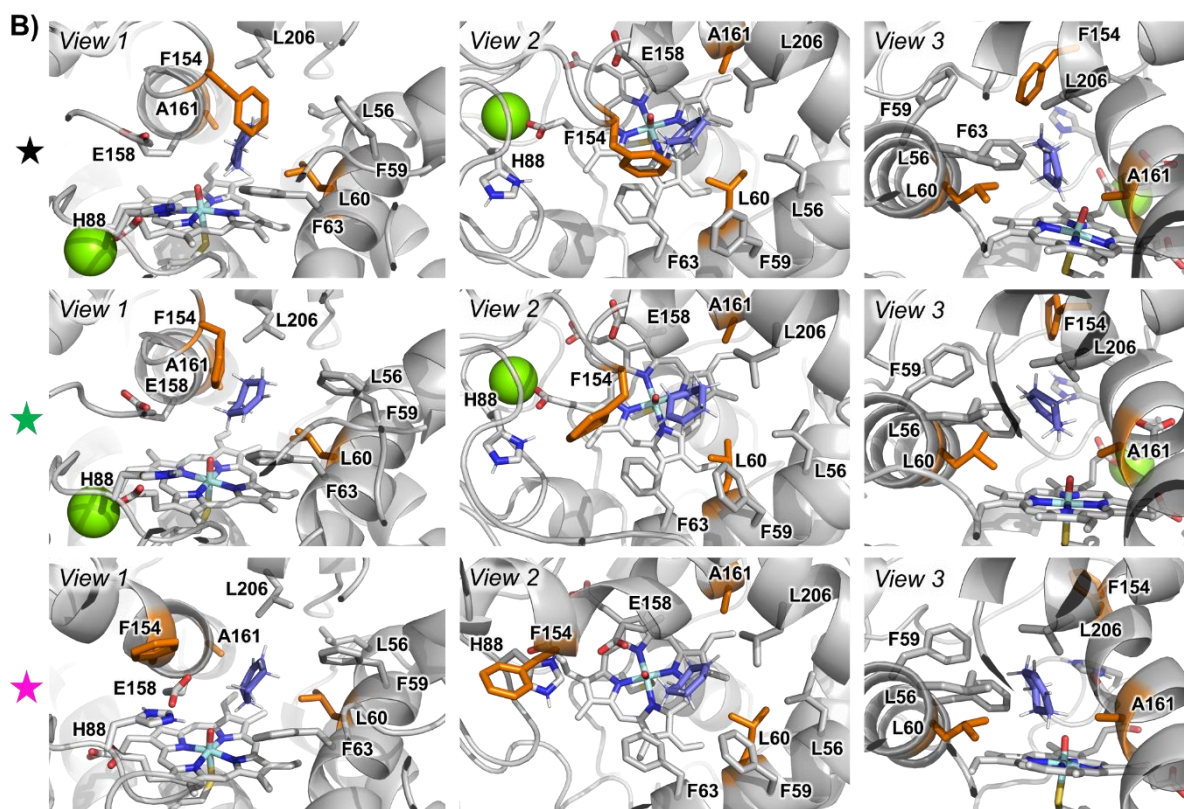


Figure S20. Analysis of cyclohexene binding poses in WT MthUPO through MD simulations. Fe=O – C(=C- cyclohexene) distance and dihedral of attack (O-C1=C1'-C2) are used as geometric parameters to characterize near attack conformations for effective cyclohexene epoxidation in heat maps. Fe=O – H(-C-cyclohexene) distance and angle of attack (O-H-C) are used to characterize near attack conformations for C-H cyclohexene hydroxylation. **A)** Overlay of heat maps for near attack conformations explored by cyclohexene effective for epoxidation and hydroxylations obtained from 3 independent MD simulations. Ideal geometric parameters obtained from DFT Transition State (TS) optimizations are shown. **B)** Representative structures from MD trajectories (highlighted with an “star” symbol) that describe reactive near attack conformations explored during MDs are shown. Distances and angles are given in angstroms (Å) and degrees ($^{\circ}$), respectively.

MD simulations show that cyclohexene binding poses that could lead to C3 hydroxylation over C2. However, it also explores near attack conformations that could lead to effective epoxidation. The preferential formation of the epoxide product by *MthUPO* WT is proposed to be because the intrinsic epoxidation barriers are lower than C-H abstraction ones (see **Figure S13**). See **Figure S19** for a comparison between cyclohexene binding poses explored in different studied *MthUPO* variants.

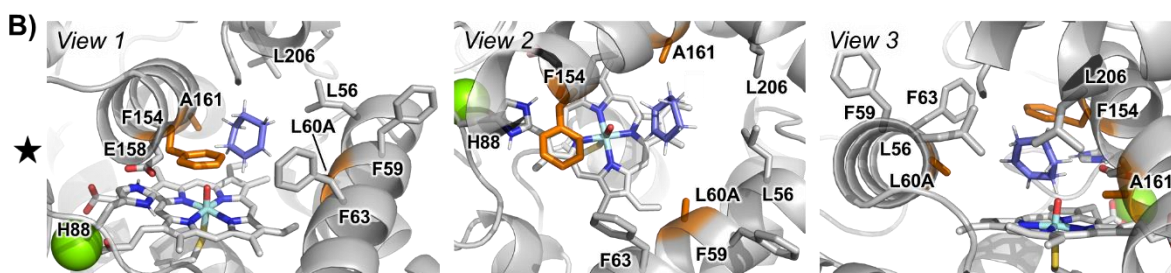
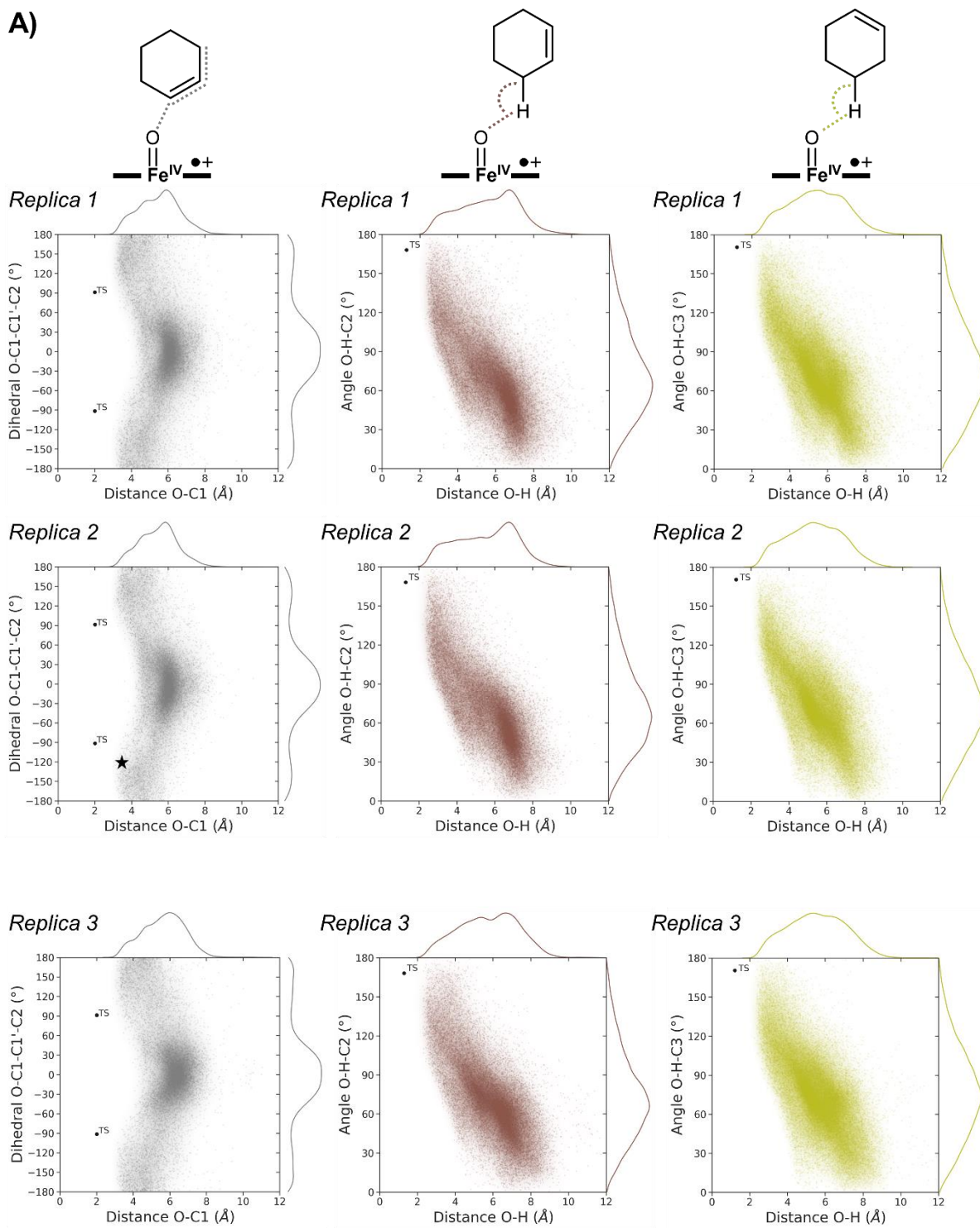
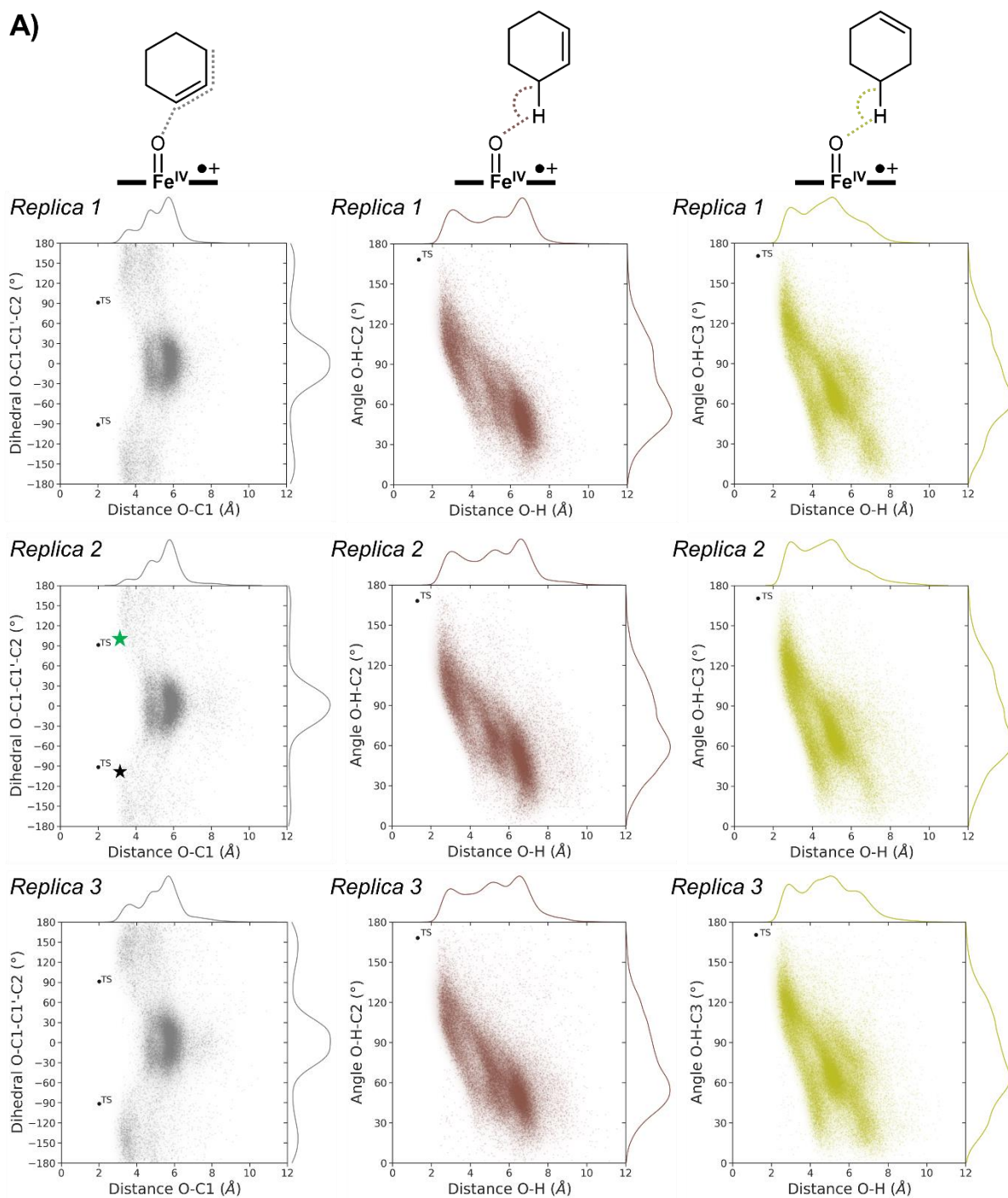


Figure S21. Analysis of cyclohexene binding poses in L60A MthUPO through MD simulations. Fe=O – C(=C- cyclohexene) distance and dihedral of attack (O-C1=C1'-C2) are used as geometric parameters to characterize near attack conformations for effective cyclohexene epoxidation in heat maps. Fe=O – H(-C-cyclohexene) distance and angle of attack (O-H-C) are used to characterize near attack conformations for C-H cyclohexene hydroxylation. **A)** Overlay of heat maps for near attack conformations explored by cyclohexene effective for epoxidation and hydroxylations obtained from 3 independent MD simulations. Ideal geometric parameters obtained from DFT Transition State (TS) optimizations are shown. **B)** Representative structures from MD trajectories (highlighted with an “star” symbol) that describe reactive near attack conformations explored during MDs are shown. Distances and angles are given in angstroms (Å) and degrees (°), respectively.

MD simulation show that cyclohexene can explore catalytically competent binding poses for epoxidation in L60A variant. This is in contrast to octane when it is bound in L60A variant (**Figure S17**). See **Figure S19** for a comparison between cyclohexene binding poses explored in different studied MthUPO variants.

A)

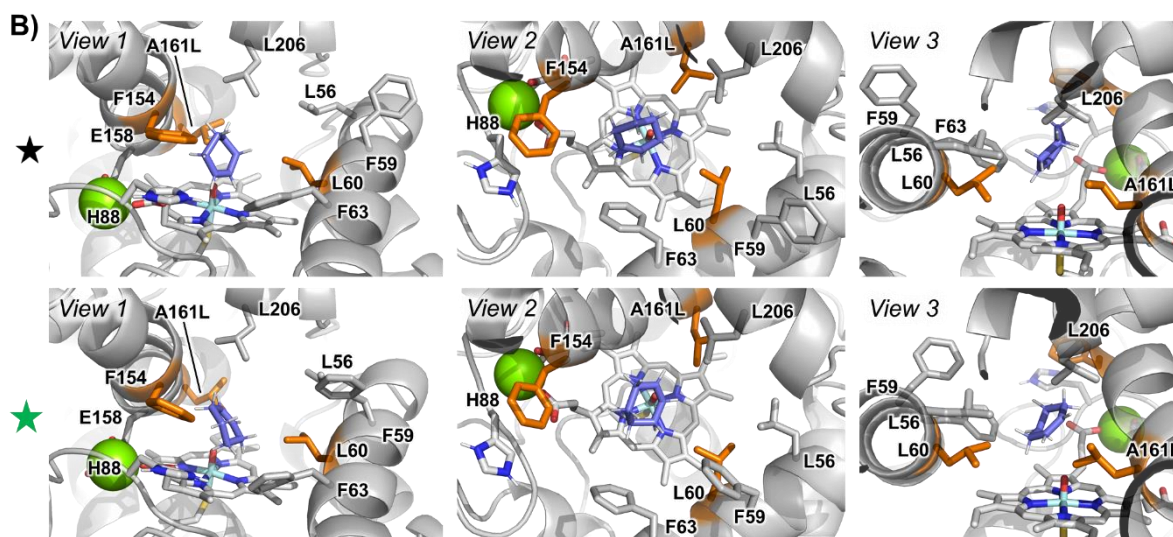


Figure S22. Analysis of cyclohexene binding poses in A161L MthUPO through MD simulations. Fe=O – C(=C- cyclohexene) distance and dihedral of attack (O-C1=C1'-C2) are used as geometric parameters to characterize near attack conformations for effective cyclohexene epoxidation in heat maps. Fe=O – H(-C-cyclohexene) distance and angle of attack (O-H-C) are used to characterize near attack conformations for C-H cyclohexene hydroxylation. **A)** Overlay of heat maps for near attack conformations explored by cyclohexene effective for epoxidation and hydroxylations obtained from 3 independent MD simulations. Ideal geometric parameters obtained from DFT Transition State (TS) optimizations are shown. **B)** Representative structures from MD trajectories (highlighted with an “star” symbol) that describe reactive near attack conformations explored during MDs are shown. Distances and angles are given in angstroms (Å) and degrees ($^{\circ}$), respectively.

Analysis of MD simulations and heat maps show that cyclohexene preferentially binds in a different conformation in A161L variant as compared to WT (see **Figure SX8** for discussion), which still allows it to better explore near attack conformations for epoxidation than in WT. See **Figure S19** for a comparison between cyclohexene binding poses explored in different studied MthUPO variants.

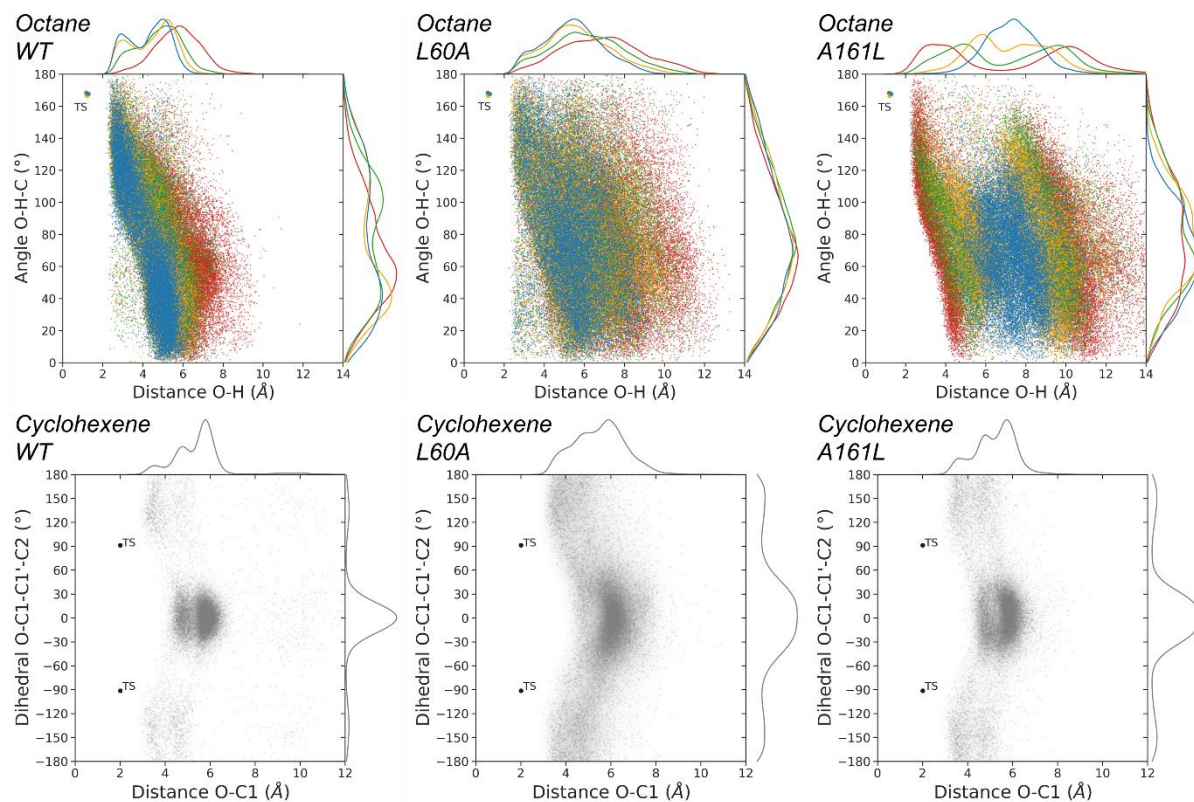


Figure S23. Comparison of near attack conformations in terms of heat maps obtained from MD simulations by octane (for hydroxylation) and cyclohexene (for epoxidation) in *MthUPO* WT, L60A, and A161L variants. See further details in Figures S16-S18, and S20-S22.

Octane binding mode in L60A is clearly much more flexible than its binding into WT and A161L variant, but also as compared to cyclohexene binding into this variant. This loose binding of octane in L60A is translated into a dramatic decrease of the enzymatic activity because near attack conformations (i.e. geometric parameters similar to TS ones) are barely explored.

Table S7. Energies and thermochemistry parameters (at T = 298.15 K and P = 1 atm) of all computationally characterized stationary points reported in **Figure S12 to S14**. Electronic energies (E), electronic energies from high level single point calculations (E (SP)), enthalpy (H), free energy (G), quasi harmonic corrected free energy (qh-G). All energies are given in a.u.

Structure	Electronic State	E	H	G	qh-G	E (SP)	Imag. Frequency
Cyclohexane	Closed-Shell Singlet	-235.880586	-235.703060	-235.738486	-235.742543	-235.993240	-
Cyclohexene	Closed-Shell Singlet	-234.649062	-234.495910	-234.530993	-234.534508	-234.760882	-
Octane	Closed-Shell Singlet	-315.713175	-315.454305	-315.503485	-315.509593	-315.866273	-
Heme Compound I	Doublet (d)	-1625.618302	-1625.277051	-1625.351712	-1625.352310	-2766.024708	-
	Quartet (q)	-1625.618014	-1625.276745	-1625.351958	-1625.352530	-2766.024374	-
TS HAT cyclohexane	Doublet (d)	-1861.461160	-1860.947392	-1861.040627	-1861.039520	-3001.992968	888.9i
	Quartet (q)	-1861.458900	-1860.945665	-1861.038451	-1861.037665	-3001.998469	1774.1i
TS CO formation cyclohexene	Doublet (d)	-1860.239763	-1859.745341	-1859.837627	-1859.836794	-3000.374267	428.5i
	Quartet (q)	-1860.238587	-1859.744063	-1859.834036	-1859.833996	-3000.776145	440.6i
TS C2-HAT cyclohexene	Doublet (d)	-1860.232957	-1859.744269	-1859.837188	-1859.836199	-3000.765330	1737.8i
	Quartet (q)	-1860.233800	-1859.744537	-1859.836661	-1859.836027	-3000.771618	1779.1i
TS C3-HAT cyclohexene	Doublet (d)	-1860.223859	-1859.735755	-1859.828459	-1859.827661	-3000.754414	1740.1i
	Quartet (q)	-1860.226407	-1859.737751	-1859.828922	-1859.828609	-3000.766647	1796.4i
TS C1-HAT octane	Doublet (d)	-1941.287481	-1940.692585	-1940.798644	-1940.797179	-3081.858611	1256.4i
	Quartet (q)	-1941.285515	-1940.691006	-1940.796932	-1940.795640	-3081.866044	1769.7i
TS C2-HAT (conformer 1) octane	Doublet (d)	-1941.291191	-1940.695782	-1940.802407	-1940.800702	-3081.865086	845.6i
	Quartet (q)	-1941.290454	-1940.695565	-1940.802449	-1940.800881	-3081.869767	1672.5i
TS C2-HAT (conformer 2) octane	Doublet (d)	-1941.285678	-1940.691215	-1940.795853	-1940.794734	-3081.868930	1222.2i
	Quartet (q)	-1941.289601	-1940.695231	-1940.800165	-1940.799187	-3081.874272	1792.8i

TS C3-HAT octane	Doublet (d)	-1941.286740	-1940.692800	-1940.797365	-1940.796649	-3081.867130	1692.7i
	Quartet (q)	-1941.286924	-1940.692628	-1940.797423	-1940.796604	-3081.874051	1850.7i
TS C4-HAT octane	Doublet (d)	-1941.289919	-1940.695091	-1940.799946	-1940.798981	-3081.877729	1144.0i
	Quartet (q)	-1941.287001	-1940.692600	-1940.796928	-1940.796306	-3081.874795	1857.0i

Table S8. Cartesian coordinates (xyz, in Å) of all DFT optimized structures.

Cyclohexane				H	-4.569644	-0.901480	-0.884625
C	1.145942	-0.916213	-0.229450	C	3.191123	-0.541507	-0.000197
C	1.366497	0.534258	0.229460	H	3.165498	-1.202545	0.877952
C	0.220537	1.450432	-0.229465	H	3.165513	-1.201896	-0.878831
C	-1.145934	0.916215	0.229467	C	4.499307	0.256370	0.000114
C	-1.366502	-0.534249	-0.229456	H	4.569676	0.900778	0.885349
C	-0.220541	-1.450438	0.229444	H	5.372893	-0.405885	-0.000222
H	0.375567	2.470160	0.146485	H	4.569614	0.901578	-0.884547
H	1.429294	0.558798	1.327822	Heme Compound I (d)			
H	2.327082	0.909822	-0.146632	Fe	0.090698	0.039631	-0.382201
H	1.198643	-0.958313	-1.327809	N	1.829229	-0.964830	-0.139477
H	1.951471	-1.560322	0.146662	N	-0.905705	-1.720414	-0.266753
H	-1.198592	0.958298	1.327829	N	1.070178	1.783261	-0.140489
H	-1.951478	1.560330	-0.146600	N	-1.665056	1.024828	-0.291510
H	-2.327079	-0.909820	0.146650	C	3.087245	-0.419024	-0.031153
H	-1.429318	-0.558777	-1.327816	C	-2.270436	-1.901928	-0.324569
H	-0.230675	-1.516985	1.327797	C	2.014257	-2.323468	-0.201842
H	-0.375566	-2.470146	-0.146562	C	-0.356318	-2.987251	-0.310478
H	0.230655	1.516927	-1.327823	C	2.425838	1.959807	-0.029070
Cyclohexene				C	-2.922178	0.480291	-0.359322
C	-1.499182	-0.047656	-0.110547	C	0.529414	3.043717	-0.176822
C	-0.666546	-1.306549	-0.056886	C	-1.844897	2.389040	-0.314662
C	0.666582	-1.306532	0.056887	C	4.084737	-1.460589	-0.012541
C	1.499184	-0.047617	0.110546	C	-2.585276	-3.308820	-0.372004
C	0.698126	1.192537	-0.318736	C	3.418908	-2.642822	-0.125944
C	-0.698159	1.192520	0.318737	C	-1.400775	-3.979243	-0.369338
H	1.200665	-2.255017	0.112171	C	2.748218	3.365000	0.010642
H	-1.200607	-2.255046	-0.112172	C	-3.919224	1.521108	-0.414372
H	-1.888799	0.090244	-1.131981	C	1.568639	4.039439	-0.085567
H	-2.387301	-0.164324	0.526026	C	-3.249759	2.706765	-0.388034
H	1.888800	0.090290	1.131979	H	5.150011	-1.289694	0.073876
H	2.387305	-0.164261	-0.526030	H	-3.589217	-3.711532	-0.410426
H	1.244672	2.105757	-0.053534	H	3.822571	-3.646791	-0.148940
H	0.592503	1.193216	-1.412754	H	-1.229838	-5.047512	-0.402137
H	-0.592537	1.193203	1.412755	H	3.750398	3.763753	0.100753
H	-1.244727	2.105726	0.053533	H	-4.986451	1.347888	-0.464425
Octane				H	1.398606	5.108331	-0.089070
C	1.940078	0.346471	0.000102	H	-3.652139	3.711256	-0.411604
H	1.966340	1.008301	-0.878678	C	3.368271	0.938290	0.033659
H	1.966391	1.007853	0.879216	C	-3.210306	-0.881943	-0.362928
C	0.625441	-0.444185	-0.000016	C	-0.828310	3.332118	-0.263398
H	0.600310	-1.105732	0.878870	C	0.999178	-3.270000	-0.297689
H	0.600369	-1.105658	-0.878961	H	4.410527	1.227823	0.122878
C	-0.625441	0.444183	-0.000060	H	-4.255525	-1.169430	-0.417329
H	-0.600307	1.105803	0.878774	H	-1.116120	4.378439	-0.284361
H	-0.600369	1.105583	-0.879057	H	1.292719	-4.313840	-0.343745
C	-1.940079	-0.346471	0.000098	O	0.164938	0.045676	-2.006475
H	-1.966388	-1.007846	0.879217	S	-0.029310	-0.376161	2.204153
H	-1.966345	-1.008309	-0.878677	C	-1.711713	-0.039643	2.806787
C	-3.191123	0.541508	-0.000170	H	-2.416897	-0.728079	2.325556
H	-3.165495	1.202504	0.878010	H	-1.742668	-0.218321	3.885694
H	-3.165516	1.201939	-0.878774	H	-2.018278	0.985493	2.585313
C	-4.499307	-0.256369	0.000102	Heme Compound I (q)			
H	-4.569646	-0.900874	0.885271	Fe	0.089058	0.036357	-0.383281
H	-5.372892	0.405887	-0.000126	N	1.837681	-0.949243	-0.143454
				N	-0.888142	-1.728201	-0.270801
				N	1.052886	1.792509	-0.134442
				N	-1.675928	1.006948	-0.293171

C	3.090242	-0.390475	-0.031935
C	-2.252140	-1.923076	-0.323078
C	2.036887	-2.305623	-0.205846
C	-0.326999	-2.990751	-0.309300
C	2.406465	1.981945	-0.024673
C	-2.927673	0.451700	-0.363358
C	0.499847	3.047262	-0.170831
C	-1.867839	2.369882	-0.313792
C	4.098047	-1.422069	-0.013411
C	-2.553125	-3.332908	-0.363727
C	3.444510	-2.610909	-0.128911
C	-1.362379	-3.992136	-0.361264
C	2.715609	3.390261	0.014535
C	-3.934179	1.483299	-0.419464
C	1.529454	4.053231	-0.080632
C	-3.275476	2.674859	-0.389785
H	5.161386	-1.240464	0.075000
H	-3.553243	-3.745289	-0.398295
H	3.858321	-3.610740	-0.152000
H	-1.181510	-5.058874	-0.390221
H	3.714019	3.798631	0.103227
H	-4.999685	1.300433	-0.471740
H	1.349001	5.120417	-0.084640
H	-3.686934	3.675691	-0.412454
C	3.358463	0.969015	0.036703
C	-3.202429	-0.913406	-0.365083
C	-0.860687	3.322517	-0.257604
C	1.030632	-3.261759	-0.300020
H	4.397976	1.267935	0.127065
H	-4.244618	-1.211833	-0.418458
H	-1.158607	4.366037	-0.276934
H	1.333199	-4.303070	-0.344553
O	0.172073	0.073905	-2.006923
S	-0.025429	-0.375115	2.199312
C	-1.711038	-0.055592	2.802305
H	-2.409898	-0.749776	2.320120
H	-1.740152	-0.236540	3.880904
H	-2.027142	0.967065	2.582807

H	-2.139371	-3.328230	2.902558
H	-1.600228	4.067316	2.664546
H	-2.837257	-0.888998	3.864155
C	1.465074	3.316285	-0.700514
C	-0.125435	-3.152201	0.898611
C	-1.453548	1.217670	2.546933
C	3.157268	-1.041040	-1.972428
H	1.679461	4.339596	-0.990987
H	-0.426126	-4.173599	1.107705
H	-2.143347	1.570231	3.306762
H	3.922919	-1.399493	-2.652792
O	-0.393079	0.104490	-1.191119
S	2.428123	0.218280	1.798363
C	2.579243	-1.405253	2.629386
H	2.907122	-2.183081	1.935528
H	3.335500	-1.290783	3.413032
H	1.636061	-1.705858	3.092464
H	-1.673498	-0.110903	-0.960850
C	-4.756422	-1.339145	-2.273849
C	-5.463313	0.023734	-2.326315
C	-5.097233	0.897663	-1.117158
C	-3.563939	1.067490	-0.990962
C	-2.895796	-0.296296	-0.949146
C	-3.222881	-1.172743	-2.146150
H	-5.569327	1.885154	-1.196841
H	-5.175312	0.545749	-3.250498
H	-6.550827	-0.118506	-2.371870
H	-5.129399	-1.911353	-1.412447
H	-4.987101	-1.928919	-3.170082
H	-3.196481	1.630454	-1.860206
H	-3.317123	1.650174	-0.096049
H	-3.058080	-0.812996	0.004260
H	-2.837874	-0.703087	-3.061839
H	-2.740155	-2.152719	-2.055162
H	-5.485111	0.433206	-0.199335

TS HAT cyclohexane (q)

TS HAT cyclohexane (d)

Fe	0.716692	0.076601	0.162835
N	2.042972	0.962447	-1.092846
N	1.410834	-1.735224	-0.384532
N	0.131821	1.902865	0.805542
N	-0.526788	-0.787603	1.456349
C	2.172645	2.306641	-1.338230
C	0.904569	-2.955490	-0.010869
C	2.962147	0.330680	-1.892961
C	2.417307	-1.992813	-1.284045
C	0.531016	3.118674	0.308030
C	-0.768915	-2.137590	1.594092
C	-0.771110	2.171094	1.803666
C	-1.345185	-0.154250	2.367159
C	3.198480	2.528582	-2.329304
C	1.619869	-4.013345	-0.681955
C	3.692574	1.305614	-2.667229
C	2.563331	-3.417257	-1.462666
C	-0.141259	4.183262	1.013189
C	-1.770323	-2.354879	2.605650
C	-0.942462	3.596585	1.945216
C	-2.118986	-1.129226	3.090751
H	3.493399	3.502534	-2.698380
H	1.414829	-5.068718	-0.555666
H	4.474874	1.064535	-3.375477
H	3.291127	-3.880935	-2.116138
H	-0.000163	5.237143	0.810056

Fe	0.763362	0.089714	0.128915
N	2.081599	0.881465	-1.141041
N	1.390319	-1.754021	-0.349122
N	0.244210	1.938784	0.766405
N	-0.565322	-0.714619	1.465429
C	2.288819	2.218812	-1.388672
C	0.852067	-2.946585	0.080789
C	2.971184	0.205423	-1.942243
C	2.367575	-2.081982	-1.255899
C	0.701320	3.130065	0.265821
C	-0.827264	-2.045281	1.655013
C	-0.697698	2.257797	1.718513
C	-1.396450	-0.032745	2.319352
C	3.317360	2.385556	-2.389719
C	1.525360	-4.050491	-0.558113
C	3.743260	1.139220	-2.728921
C	2.469354	-3.515106	-1.381662
C	0.049032	4.231932	0.929764
C	-1.860204	-2.212765	2.651320
C	-0.817006	3.690736	1.831775
C	-2.210791	-0.963218	3.065746
H	3.661143	3.342198	-2.761843
H	1.291579	-5.093553	-0.386926
H	4.508620	0.856039	-3.440121
H	3.169191	-4.026593	-2.029989
H	0.238480	5.276347	0.717349
H	-2.247551	-3.167986	2.982145
H	-1.487441	4.198872	2.513052
H	-2.947534	-0.679169	3.806319

C	1.649726	3.266974	-0.743562
C	-0.176869	-3.089397	1.002512
C	-1.459957	1.349896	2.443158
C	3.120896	-1.172656	-1.990368
H	1.919921	4.275541	-1.040143
H	-0.489231	-4.100468	1.244705
H	-2.169127	1.755190	3.158123
H	3.864946	-1.573370	-2.671402
O	-0.465205	0.082797	-1.126096
S	2.212423	0.196559	1.995782
C	2.681055	-1.483082	2.532182
H	3.185803	-2.032247	1.734353
H	3.349773	-1.379882	3.392133
H	1.794376	-2.042275	2.846682
H	-1.635006	-0.102833	-0.881438
C	-4.797744	-1.348902	-2.215599
C	-5.453877	0.029441	-2.390161
C	-5.113144	0.971380	-1.225046
C	-3.581046	1.098418	-1.036872
C	-2.961096	-0.275985	-0.879852
C	-3.265968	-1.221092	-2.025545
H	-5.547827	1.965333	-1.392980
H	-5.105431	0.478925	-3.331690
H	-6.542553	-0.080601	-2.479205
H	-5.228791	-1.849698	-1.336918
H	-5.009865	-1.989354	-3.081542
H	-3.158272	1.594098	-1.922541
H	-3.355167	1.731858	-0.171067
H	-3.139862	-0.720872	0.105022
H	-2.827080	-0.828961	-2.954086
H	-2.821928	-2.208019	-1.849100
H	-5.558700	0.582139	-0.298387

C	-1.070666	3.136792	-0.434003
C	-1.532842	-1.060950	-2.820375
C	2.675059	1.306554	2.028478
H	2.418010	-3.976617	0.000497
H	-1.583990	4.092673	-0.461262
H	-2.166596	-1.418189	-3.625767
H	3.365308	1.690197	2.773053
O	-0.551498	-0.360097	1.025371
S	2.147388	0.692520	-1.910815
C	1.678579	2.284433	-2.684193
H	1.616381	3.085251	-1.942318
H	2.464929	2.539355	-3.403071
H	0.726515	2.212687	-3.216106
C	-2.184530	-2.280780	2.419765
C	-2.407606	-1.619727	1.088578
C	-3.195841	-0.511841	0.940121
C	-3.809045	0.218371	2.096700
C	-3.835276	-0.622340	3.384806
C	-2.499467	-1.347656	3.598604
H	-3.358799	-0.110471	-0.056588
H	-2.061677	-2.143658	0.203712
H	-2.825130	-3.177038	2.465452
H	-1.152714	-2.646652	2.472773
H	-3.232972	1.144863	2.260430
H	-4.820019	0.552373	1.825832
H	-4.068999	0.018915	4.242585
H	-4.643303	-1.363927	3.314673
H	-1.694711	-0.607380	3.689875
H	-2.518772	-1.920301	4.533328

TS C-O formation cyclohexene (q)

TS C-O formation cyclohexene (d)

Fe	0.437445	0.072264	-0.261265
N	2.023921	-0.687148	0.749225
N	0.761735	1.876676	0.596798
N	0.243544	-1.679368	-1.244516
N	-0.992595	0.878658	-1.408190
C	2.465642	-1.986071	0.730329
C	0.000027	3.006898	0.441473
C	2.803075	-0.028158	1.666883
C	1.714172	2.180398	1.538346
C	0.939980	-2.838776	-1.008581
C	-1.513095	2.148032	-1.303641
C	-0.627235	-1.957672	-2.269866
C	-1.703133	0.254263	-2.406753
C	3.559459	-2.150877	1.658844
C	0.489378	4.057721	1.303161
C	3.771845	-0.936206	2.235398
C	1.555672	3.547010	1.978042
C	0.486672	-3.879446	-1.900344
C	-2.579277	2.324669	-2.258005
C	-0.480794	-3.331525	-2.686631
C	-2.691666	1.154300	-2.947155
H	4.085927	-3.081494	1.828164
H	0.062639	5.050740	1.364099
H	4.506989	-0.660450	2.980636
H	2.185998	4.031501	2.712783
H	0.878076	-4.888634	-1.914293
H	-3.150425	3.236514	-2.377523
H	-1.052973	-3.796708	-3.479125
H	-3.376644	0.903843	-3.747131
C	1.961064	-2.995339	-0.079141
Fe	0.476567	0.034280	-0.272054
N	1.960952	-0.870895	0.717758
N	0.994516	1.792247	0.531313
N	0.057955	-1.700803	-1.240765
N	-0.987486	0.964052	-1.355071
C	2.277955	-2.209319	0.686938
C	0.339997	2.994676	0.378995
C	2.852216	-0.287878	1.584346
C	2.015216	2.023173	1.420754
C	0.640461	-2.919944	-1.018032
C	-1.369816	2.273935	-1.251431
C	-0.904645	-1.902910	-2.203130
C	-1.817798	0.391286	-2.285410
C	3.388310	-2.475949	1.572819
C	0.978021	4.008716	1.183394
C	3.747779	-1.285351	2.123976
C	2.019688	3.408861	1.823554
C	0.041157	-3.920624	-1.868084
C	-2.481970	2.539917	-2.135859
C	-0.914767	-3.288861	-2.605405
C	-2.757499	1.371571	-2.779953
H	3.827243	-3.453240	1.728762
H	0.656805	5.041217	1.236715
H	4.541793	-1.078766	2.830226
H	2.729711	3.844697	2.514789
H	0.327623	-4.964490	-1.885297
H	-2.968046	3.501480	-2.242005
H	-1.578411	-3.706956	-3.351574
H	-3.518687	1.172860	-3.523724
C	1.666742	-3.166390	-0.109313
C	-0.760162	3.223578	-0.435821
C	-1.777627	-0.937690	-2.691565
C	2.894921	1.062038	1.904593
H	2.032358	-4.185696	-0.034540

H	-1.166224	4.230201	-0.452226
H	-2.495746	-1.251417	-3.442804
H	3.656648	1.387848	2.605770
O	-0.632781	-0.310601	0.998025
S	1.839154	0.399582	-2.201335
C	2.056033	2.193216	-2.474982
H	2.537323	2.674373	-1.620236
H	2.680744	2.319341	-3.364937
H	1.090729	2.674366	-2.658948
C	-2.324045	-2.045623	2.149144
C	-2.500004	-1.058156	1.022292
C	-3.228209	0.106888	1.202750
C	-3.605533	0.629188	2.556642
C	-3.632222	-0.470192	3.633736
C	-2.399327	-1.378880	3.530051
H	-3.458750	0.720576	0.335483
H	-2.396002	-1.444551	0.015032
H	-3.123842	-2.798540	2.056723
H	-1.379187	-2.583493	2.019344
H	-2.879232	1.409955	2.843305
H	-4.574314	1.143559	2.499605
H	-3.694139	-0.013849	4.628735
H	-4.539872	-1.076842	3.506727
H	-1.491102	-0.783912	3.689970
H	-2.423177	-2.146349	4.313024

TS C2-HAT cyclohexene (d)

Fe	0.581231	0.009799	0.200785
N	1.819868	1.196786	-0.867095
N	1.465282	-1.615653	-0.639584
N	-0.170560	1.610096	1.155890
N	-0.520955	-1.190351	1.385865
C	1.808582	2.568963	-0.885436
C	1.099506	-2.928319	-0.448979
C	2.748887	0.815417	-1.799273
C	2.454031	-1.633182	-1.592933
C	0.104027	2.925276	0.877630
C	-0.606250	-2.558435	1.306763
C	-1.052584	1.625203	2.205534
C	-1.363673	-0.818252	2.407134
C	2.764288	3.066005	-1.847679
C	1.892411	-3.793639	-1.292126
C	3.352458	1.975231	-2.412826
C	2.737858	-2.992060	-1.995364
C	-0.638631	3.791877	1.762267
C	-1.534442	-3.059570	2.292807
C	-1.351926	2.982697	2.594198
C	-1.996332	-1.979828	2.983529
H	2.948544	4.113739	-2.048231
H	1.801510	-4.871848	-1.324287
H	4.119159	1.940170	-3.176157
H	3.482554	-3.273987	-2.728663
H	-0.596603	4.873377	1.743346
H	-1.777718	-4.105027	2.432822
H	-2.021794	3.260807	3.397777
H	-2.701720	-1.953906	3.804177
C	1.008858	3.373675	-0.080937
C	0.123644	-3.364551	0.436231
C	-1.598520	0.492355	2.805452
C	3.064139	-0.502754	-2.124735
H	1.116145	4.448155	-0.194032
H	-0.061488	-4.433395	0.481904
H	-2.282972	0.647115	3.633803
H	3.827405	-0.658448	-2.880979
O	-0.569579	0.026731	-1.111370
S	2.305444	-0.390050	1.925732

C	3.956795	0.035444	1.283067
H	4.012654	1.085960	0.986695
H	4.694182	-0.168857	2.065347
H	4.196445	-0.587382	0.413695
C	-3.062665	0.345474	-0.700925
C	-3.697135	-0.971915	-0.844566
C	-4.555283	-1.276299	-1.841189
C	-5.039335	-0.253596	-2.837682
C	-4.847255	1.176726	-2.307658
C	-3.415829	1.372279	-1.777375
H	-4.957659	-2.285544	-1.914852
H	-3.438632	-1.732475	-0.108845
H	-3.074675	0.726110	0.326263
H	-1.796444	0.149385	-0.820122
H	-4.498902	-0.374552	-3.790805
H	-6.096282	-0.437317	-3.072474
H	-5.061072	1.908277	-3.096286
H	-5.566060	1.357388	-1.496858
H	-2.718142	1.264767	-2.619842
H	-3.280091	2.388192	-1.389664

TS C2-HAT cyclohexene (q)

Fe	0.686232	0.034425	0.130805
N	2.018577	0.871166	-1.103259
N	1.184826	-1.779400	-0.542122
N	0.299807	1.847484	0.964640
N	-0.618314	-0.813626	1.460412
C	2.294173	2.212240	-1.230387
C	0.598942	-2.977497	-0.196392
C	2.832957	0.228920	-2.003110
C	2.106152	-2.074613	-1.517942
C	0.813556	3.051737	0.560533
C	-0.942569	-2.140738	1.545861
C	-0.578853	2.127297	1.984366
C	-1.367494	-0.172106	2.417714
C	3.294819	2.418735	-2.252318
C	1.179240	-4.051247	-0.965193
C	3.631888	1.189696	-2.728089
C	2.117479	-3.493030	-1.779378
C	0.256299	4.121840	1.352095
C	-1.927322	-2.348868	2.582816
C	-0.606652	3.547678	2.236384
C	-2.189125	-1.126559	3.124541
H	3.681631	3.386502	-2.545004
H	0.893450	-5.091735	-0.878169
H	4.351892	0.935197	-3.495256
H	2.759738	-3.978591	-2.502848
H	0.503525	5.168840	1.231922
H	-2.345909	-3.310727	2.850301
H	-1.216217	4.025493	2.992659
H	-2.869872	-0.875538	3.927921
C	1.737851	3.227708	-0.465489
C	-0.388796	-3.151302	0.763507
C	-1.354722	1.194857	2.664376
C	2.888782	-1.145080	-2.192625
H	2.059750	4.242800	-0.675937
H	-0.745788	-4.162735	0.930543
H	-2.005698	1.566667	3.449474
H	3.579616	-1.521242	-2.940468
O	-0.567057	0.225622	-1.050603
S	2.236966	-0.091461	1.939631
C	2.586697	-1.838514	2.333690
H	3.023293	-2.361231	1.479466
H	3.286023	-1.856359	3.175130
H	1.668688	-2.352989	2.634993
C	-3.078916	0.577301	-0.678237

C	-3.758577	-0.718869	-0.659811
C	-4.590474	-1.134916	-1.643326
C	-4.997503	-0.245598	-2.789351
C	-4.787250	1.237860	-2.444214
C	-3.372829	1.470732	-1.885431
H	-5.027695	-2.130748	-1.591860
H	-3.561524	-1.375041	0.186405
H	-3.075942	1.086235	0.292525
H	-1.815828	0.329523	-0.752675
H	-4.416078	-0.505944	-3.689141
H	-6.046886	-0.435873	-3.050604
H	-4.950630	1.862753	-3.330418
H	-5.531857	1.539219	-1.694990
H	-2.646542	1.249631	-2.680310
H	-3.228967	2.523892	-1.619096

TS C3-HAT cyclohexene (d)

Fe	-0.458121	0.121748	-0.246167
N	-0.839367	2.083341	0.024955
N	-1.941422	-0.324240	1.056100
N	0.898709	0.557678	-1.675278
N	-0.239804	-1.837285	-0.697559
C	-0.175523	3.129016	-0.559269
C	-2.326312	-1.575556	1.451708
C	-1.738533	2.646306	0.892539
C	-2.693425	0.553449	1.798251
C	1.317704	1.816350	-2.039694
C	-0.881988	-2.888939	-0.080083
C	1.612873	-0.313800	-2.460308
C	0.630805	-2.408372	-1.603650
C	-0.671349	4.387112	-0.052971
C	-3.348880	-1.492309	2.470042
C	-1.646240	4.086205	0.849993
C	-3.579641	-0.167490	2.682911
C	2.327632	1.732077	-3.068053
C	-0.415244	-4.143913	-0.620026
C	2.510210	0.408271	-3.330050
C	0.520321	-3.845724	-1.563270
H	-0.311004	5.360633	-0.359777
H	-3.819317	-2.345003	2.942664
H	-2.252939	4.760590	1.440581
H	-4.277465	0.295867	3.368479
H	2.815205	2.584590	-3.523347
H	-0.768268	-5.117419	-0.304596
H	3.179725	-0.053434	-4.044383
H	1.094252	-4.523429	-2.182185
C	0.827201	3.008146	-1.519187
C	-1.837952	-2.769804	0.921622
C	1.496659	-1.701337	-2.424336
C	-2.611848	1.937692	1.714663
H	1.257253	3.928504	-1.902755
H	-2.246865	-3.691771	1.324056
H	2.129936	-2.273570	-3.095237
H	-3.270683	2.516017	2.355269
O	0.676508	0.101558	1.109576
S	-2.064123	-0.069435	-2.184370
C	-3.611215	-0.863575	-1.640561
H	-4.088167	-0.305360	-0.831360
H	-4.288327	-0.928112	-2.497797
H	-3.403686	-1.881744	-1.290677
C	3.187847	-1.762291	1.902173
C	3.355055	-1.218950	3.300166
C	3.548639	0.076065	3.573607
C	3.643032	1.147355	2.514422
C	3.912706	0.558407	1.118285
C	3.071092	-0.672913	0.851539

H	3.637729	0.397031	4.611116
H	3.305050	-1.941682	4.113870
H	4.047161	-2.414150	1.658425
H	2.312350	-2.425921	1.859349
H	2.706998	1.724634	2.495902
H	4.433514	1.863407	2.776701
H	3.748099	1.315392	0.342837
H	4.976359	0.270133	1.053749
H	1.790831	-0.261392	0.896318
H	3.128722	-1.046084	-0.173831

TS C3-HAT cyclohexene (q)

Fe	0.532429	0.135785	-0.253190
N	1.551515	1.619229	0.608932
N	-0.558608	1.476663	-1.303782
N	1.728576	-1.213579	0.626127
N	-0.485687	-1.380383	-1.180855
C	2.619827	1.503184	1.466631
C	-1.570599	1.208873	-2.197984
C	1.329629	2.968613	0.460667
C	-0.492160	2.841906	-1.198669
C	2.770821	-0.955946	1.481731
C	-1.508986	-1.257134	-2.088177
C	1.598718	-2.584067	0.584701
C	-0.306355	-2.723779	-0.984480
C	3.067714	2.811274	1.885771
C	-2.140760	2.442899	-2.680218
C	2.266379	3.718504	1.265817
C	-1.472640	3.455678	-2.060185
C	3.331213	-2.191576	1.970762
C	-1.992934	-2.563379	-2.469333
C	2.600474	-3.200492	1.419313
C	-1.248243	-3.474386	-1.782633
H	3.892679	2.989053	2.563662
H	-2.950930	2.506505	-3.395392
H	2.295592	4.798968	1.325396
H	-1.619710	4.523371	-2.160933
H	4.167062	-2.258403	2.655358
H	-2.796308	-2.740704	-3.172880
H	2.713807	-4.268582	1.554568
H	-1.311484	-4.554820	-1.806459
C	3.201428	0.309222	1.866628
C	-2.016437	-0.054920	-2.565437
C	0.657318	-3.289368	-0.153547
C	0.382799	3.543071	-0.374299
H	4.043271	0.364900	2.549427
H	-2.831898	-0.105631	-3.280162
H	0.683991	-4.372500	-0.086532
H	0.326265	4.626811	-0.394362
O	-0.605608	0.116805	1.084793
S	1.839622	0.137169	-2.230539
C	2.813866	-1.400618	-2.348257
H	2.148569	-2.268391	-2.395712
H	3.391337	-1.354836	-3.276586
H	3.488909	-1.514001	-1.497125
C	-3.902678	-0.038800	0.892903
C	-4.164843	0.902245	2.042984
C	-3.648023	0.740633	3.266264
C	-2.756317	-0.415045	3.650155
C	-2.840597	-1.572450	2.639660
C	-2.845038	-1.081746	1.205426
H	-3.864311	1.476298	4.040435
H	-4.808989	1.756337	1.836993
H	-4.843445	-0.550207	0.616329
H	-3.622182	0.530481	-0.004632
H	-1.716757	-0.064439	3.724245

H	-3.023913	-0.775636	4.652505
H	-2.024335	-2.285747	2.802408
H	-3.778771	-2.128072	2.812031
H	-1.658512	-0.478719	1.039531
H	-2.784207	-1.879482	0.460974

TS Cl-HAT octane (d)

Fe	-1.643496	0.033531	0.045059
N	-2.877800	0.869375	-1.332076
N	-1.033698	1.870547	0.608979
N	-2.371665	-1.790816	-0.432055
N	-0.491983	-0.783024	1.450203
C	-3.678382	0.206504	-2.228564
C	-0.041031	2.165372	1.510532
C	-3.046889	2.209135	-1.577134
C	-1.458039	3.072776	0.094261
C	-3.248937	-2.088456	-1.445712
C	0.421096	-0.132838	2.252801
C	-2.057750	-2.983489	0.170563
C	-0.434482	-2.115266	1.802367
C	-4.366371	1.156658	-3.069649
C	0.157739	3.592526	1.577321
C	-3.981011	2.397116	-2.661274
C	-0.726598	4.154759	0.707374
C	-3.492681	-3.510222	-1.482882
C	1.076895	-1.080384	3.115928
C	-2.760884	-4.063935	-0.476460
C	0.540408	-2.304115	2.844782
H	-5.056771	0.888769	-3.859160
H	0.882121	4.081728	2.215819
H	-4.285158	3.361274	-3.048050
H	-0.876479	5.202037	0.478288
H	-4.147306	-4.000791	-2.191789
H	1.839399	-0.822996	3.839846
H	-2.685177	-5.104632	-0.188520
H	0.775995	-3.259189	3.296448
C	-3.848085	-1.169422	-2.297010
C	0.656216	1.235403	2.269715
C	-1.167114	-3.141747	1.223427
C	-2.405856	3.240955	-0.905743
H	-4.523014	-1.554587	-3.054356
H	1.412839	1.606605	2.953137
H	-1.011416	-4.145508	1.605027
H	-2.637352	4.256683	-1.209446
O	-0.443569	-0.018475	-1.245379
S	-3.468566	0.186323	1.547366
C	-2.884549	0.945124	3.106484
H	-2.555838	1.975962	2.954795
H	-3.735944	0.944269	3.795215
H	-2.071854	0.365837	3.551718
C	1.689913	-1.348299	-1.073066
H	0.583978	-0.709271	-1.064435
H	1.636391	-1.885845	-2.024465
H	1.599139	-2.025149	-0.219946
C	2.805438	-0.334252	-0.974367
H	2.746204	0.367109	-1.816793
H	2.688862	0.256564	-0.056459
C	4.199857	-0.999796	-0.969535
H	4.321287	-1.594008	-1.886027
H	4.259937	-1.707017	-0.130293
C	5.342375	0.020215	-0.863564
H	5.211456	0.616369	0.051449
H	5.275113	0.727904	-1.702694
C	6.734268	-0.626170	-0.853884
H	6.798749	-1.336823	-0.016506
H	6.864650	-1.221197	-1.769927

C	7.877996	0.391098	-0.743624
H	7.747343	0.986932	0.172194
H	7.814075	1.102086	-1.580923
C	9.271387	-0.251639	-0.732716
H	9.335284	-0.962310	-0.103709
H	9.402562	-0.846019	-1.648221
C	10.407263	0.771207	-0.621168
H	10.322200	1.357854	0.302164
H	11.388143	0.281676	-0.616020
H	10.389948	1.475038	-1.462714

TS Cl-HAT octane (q)

Fe	-1.682949	0.064248	0.009913
N	-2.895442	0.919993	-1.323979
N	-1.053891	1.869530	0.614790
N	-2.439989	-1.756165	-0.443988
N	-0.475647	-0.819345	1.409231
C	-3.753548	0.280430	-2.187895
C	-0.061546	2.134312	1.531969
C	-3.046801	2.264400	-1.565984
C	-1.446338	3.087686	0.116464
C	-3.361773	-2.032525	-1.420470
C	0.424349	-0.188238	2.226593
C	-2.078133	-2.969414	-2.097238
C	-0.386376	-2.158614	1.701220
C	-4.442912	1.247363	-3.011223
C	0.157969	3.556654	1.625421
C	-4.008148	2.476343	-2.623372
C	-0.704622	4.148269	0.752551
C	-3.603419	-3.452745	-1.488928
C	1.112050	-1.154560	3.051589
C	-2.808324	-4.033107	-0.546738
C	0.606055	-2.376983	2.727381
H	-5.168947	0.996496	-3.773949
H	0.883516	4.023862	2.278990
H	-4.299843	3.447715	-3.001669
H	-0.832425	5.201503	0.537773
H	-4.291890	-3.926324	-2.177006
H	1.872538	-0.909921	3.782127
H	-2.707734	-5.082658	-0.301432
H	0.866721	-3.345548	3.134570
C	-3.973537	-1.088120	-2.239561
C	0.629916	1.188072	2.277787
C	-1.129046	-3.162862	1.093128
C	-2.385976	3.279875	-0.890203
H	-4.688214	-1.451759	-2.971112
H	1.381907	1.554312	2.969767
H	-0.949497	-4.183121	1.417343
H	-2.601956	4.302053	-1.184341
O	-0.417298	-0.057310	-1.208690
S	-3.322392	-0.042144	1.713140
C	-2.890444	1.083398	3.081657
H	-2.816917	2.118437	2.740883
H	-3.674104	0.996403	3.840304
H	-1.937643	0.785752	3.530704
C	1.726871	-1.399262	-1.069919
H	0.542856	-0.718614	-1.025397
H	1.649408	-1.898914	-2.039690
H	1.644933	-2.100189	-0.236533
C	2.831785	-0.377604	-0.954946
H	2.754590	0.349375	-1.774563
H	2.719765	0.186046	-0.018894
C	4.238002	-1.018444	-0.983850
H	4.359651	-1.581935	-1.919705
H	4.316346	-1.751646	-0.168526
C	5.367880	0.012780	-0.854978
H	5.236122	0.579104	0.078848

H	5.285291	0.745291	-1.671296
C	6.768383	-0.614574	-0.874526
H	6.847267	-1.350892	-0.060798
H	6.900444	-1.178593	-1.809812
C	7.900554	0.412383	-0.738500
H	7.768110	0.977597	0.196315
H	7.823575	1.148584	-1.552623
C	9.301479	-0.213687	-0.755039
H	9.378062	-0.949851	0.057971
H	9.434667	-0.777143	-1.689626
C	10.426181	0.818166	-0.616535
H	10.339289	1.374118	0.325445
H	11.412641	0.340154	-0.631778
H	10.396406	1.548193	-1.435107

TS C2-HAT octane (conformation 1) (d)

Fe	-1.390786	0.085715	0.092197
N	-2.528477	0.810031	-1.427141
N	-0.775379	1.955756	0.518224
N	-2.137192	-1.761353	-0.252927
N	-0.330847	-0.615890	1.627623
C	-3.300850	0.080696	-2.296651
C	0.173913	2.317302	1.442982
C	-2.652566	2.123518	-1.805872
C	-1.139861	3.110657	-0.132395
C	-2.968514	-2.136997	-1.278982
C	0.548700	0.091200	2.417836
C	-1.869514	-2.900318	0.464939
C	-0.312300	-1.912592	2.094559
C	-3.921881	0.959777	-3.258794
C	0.402405	3.740028	1.386021
C	-3.525977	2.225406	-2.950683
C	-0.418109	4.232499	0.416818
C	-3.234372	-3.553080	-1.202821
C	1.143217	-0.784486	3.394317
C	-2.558466	-4.025129	-0.118552
C	0.603689	-2.021445	3.200296
H	-4.579296	0.631254	-4.053547
H	1.101937	4.274426	2.015960
H	-3.786744	3.154169	-3.441686
H	-0.529670	5.255365	0.080780
H	-3.862670	-4.096257	-1.897031
H	1.870172	-0.473268	4.133499
H	-2.512197	-5.037369	0.262046
H	0.800065	-2.936367	3.744442
C	-3.503190	-1.291086	-2.242213
C	0.808836	1.451885	2.323032
C	-1.031039	-2.976797	1.568654
C	-2.025364	3.201646	-1.197879
H	-4.148735	-1.733290	-2.994003
H	1.535660	1.873691	3.009466
H	-0.909463	-3.945705	2.041839
H	-2.214382	4.188505	-1.607686
O	-0.139601	-0.105862	-1.117277
S	-3.290654	0.383899	1.481606
C	-2.810021	1.399172	2.926715
H	-2.529364	2.413275	2.632487
H	-3.686220	1.451656	3.581502
H	-1.986435	0.939718	3.479014
C	2.018767	-1.406444	-0.709420
H	0.950306	-0.802645	-0.800804
H	2.017047	-1.738512	0.335160
C	3.091607	-0.363325	-0.980138
H	3.003980	-0.007909	-2.016164
H	2.918969	0.505655	-0.331106
C	4.525181	-0.881521	-0.738742

H	4.725919	-1.734970	-1.400439
H	4.603793	-1.261170	0.290288
C	5.591182	0.198886	-0.967340
H	5.389005	1.053381	-0.304792
H	5.504414	0.581503	-1.994901
C	7.023173	-0.299366	-0.730585
H	7.109934	-0.682518	0.297217
H	7.225132	-1.154528	-1.392774
C	8.090914	0.779022	-0.959162
H	7.888719	1.633825	-0.298056
H	8.004513	1.161097	-1.986331
C	9.518506	0.275362	-0.720240
H	9.645217	-0.081399	0.309609
H	9.761580	-0.558068	-1.391185
H	10.256445	1.067674	-0.891839
C	1.913130	-2.564392	-1.684238
H	2.804616	-3.205133	-1.625457
H	1.043671	-3.192273	-1.461878
H	1.827896	-2.208178	-2.717452

TS C2-HAT octane (conformation 1) (q)

Fe	-1.418082	0.105341	0.029255
N	-2.539108	0.909296	-1.421993
N	-0.790388	1.935065	0.570436
N	-2.215542	-1.714489	-0.343398
N	-0.364976	-0.708513	1.582590
C	-3.380319	0.243565	-2.279338
C	0.126715	2.238082	1.549258
C	-2.613188	2.234519	-1.774519
C	-1.090283	3.123937	-0.048673
C	-3.102564	-2.026229	-1.343243
C	0.480881	-0.045710	2.434393
C	-1.904782	-2.904273	0.274120
C	-0.307012	-2.033940	1.943235
C	-3.983898	1.170754	-3.209419
C	0.393274	3.655495	1.559365
C	-3.508410	2.405946	-2.895938
C	-0.364209	4.205853	0.569632
C	-3.373933	-3.442587	-1.346241
C	1.089947	-0.974636	3.358299
C	-2.628408	-3.987557	-0.344492
C	0.601009	-2.208342	3.052676
H	-4.683363	0.892207	-3.987194
H	1.075455	4.147399	2.240865
H	-3.734221	3.356427	-3.362104
H	-0.432017	5.243201	0.267962
H	-4.044956	-3.938311	-2.035932
H	1.794088	-0.699575	4.133163
H	-2.561081	-5.024087	-0.039796
H	0.819966	-3.157476	3.524923
C	-3.649176	-1.118378	-2.244683
C	0.716918	1.325683	2.417438
C	-1.014786	-3.059647	1.330970
C	-1.945965	3.270826	-1.135106
H	-4.342464	-1.508356	-2.983340
H	1.420271	1.718502	3.145166
H	-0.868097	-4.065158	1.712893
H	-2.095073	4.274808	-1.519920
O	-0.109183	-0.113269	-1.073372
S	-3.198482	0.159841	1.687594
C	-2.839382	1.409734	2.963516
H	-2.744258	2.408139	2.530566
H	-3.657100	1.393429	3.690387
H	-1.909466	1.158434	3.484982
C	2.089086	-1.403530	-0.684536
H	0.956714	-0.778186	-0.773480

H	2.110501	-1.755132	0.353658
C	3.158805	-0.353218	-0.948865
H	3.060757	0.018083	-1.979441
H	2.987384	0.509338	-0.289461
C	4.599710	-0.858093	-0.729064
H	4.801724	-1.703078	-1.401731
H	4.691250	-1.250340	0.294610
C	5.658928	0.229741	-0.953306
H	5.457048	1.076471	-0.280373
H	5.563174	0.623656	-1.976018
C	7.095596	-0.262195	-0.732043
H	7.191073	-0.657458	0.290504
H	7.297940	-1.108593	-1.405446
C	8.157136	0.823558	-0.953987
H	7.955144	1.669537	-0.281483
H	8.062953	1.217690	-1.975950
C	9.588492	0.323744	-0.729613
H	9.722798	-0.045106	0.295037
H	9.831307	-0.500454	-1.412005
H	10.322140	1.121244	-0.895732
C	2.000267	-2.551956	-1.674960
H	2.900344	-3.183811	-1.643878
H	1.142051	-3.197922	-1.456808
H	1.894718	-2.182054	-2.702493

TS C2-HAT octane (conformation 2) (d)

Fe	-1.045683	0.243638	0.217109
N	-1.020765	2.205957	-0.322154
N	0.589978	0.528622	1.361975
N	-2.756387	-0.000807	-0.841293
N	-1.113704	-1.661207	0.799017
C	-1.904639	2.852391	-1.147487
C	1.246893	-0.404341	2.124033
C	-0.075968	3.135807	0.028730
C	1.306819	1.695217	1.487746
C	-3.414436	0.945705	-1.584722
C	-0.235855	-2.313845	1.637221
C	-3.468672	-1.160604	-0.987548
C	-2.054488	-2.601801	0.437301
C	-1.506061	4.230532	-1.324329
C	2.400511	0.187644	2.757270
C	-0.369942	4.405857	-0.596066
C	2.438603	1.490122	2.360424
C	-4.579113	0.365793	-2.212702
C	-0.625057	-3.693190	1.793701
C	-4.612236	-0.944147	-1.843159
C	-1.751891	-3.871784	1.049681
H	-2.039036	4.951824	-1.930455
H	3.081549	-0.340174	3.412486
H	0.225861	5.301850	-0.477518
H	3.157097	2.255694	2.624079
H	-5.266759	0.906453	-2.850409
H	-0.094950	-4.415502	2.401146
H	-5.332988	-1.705588	-2.112454
H	-2.339649	-4.771462	0.919426
C	-3.027210	2.273174	-1.727476
C	0.865584	-1.735281	2.254699
C	-3.143179	-2.377176	-0.396233
C	1.005129	2.902901	0.870367
H	-3.648772	2.907711	-2.351619
H	1.473425	-2.370988	2.890890
H	-3.799587	-3.219109	-0.593118
H	1.671939	3.737432	1.064127
O	-0.092761	0.005764	-1.225651
S	-2.360124	1.041035	2.051631
C	-2.171639	-0.121185	3.454953

H	-1.126092	-0.206267	3.764706
H	-2.747191	0.286616	4.292893
H	-2.556169	-1.115606	3.213686
C	0.929100	-2.170137	-1.906891
H	0.363062	-1.080518	-1.451084
H	0.956505	-2.770901	-0.992008
C	2.293820	-1.725063	-2.379113
H	2.179955	-0.973097	-3.172567
C	-0.031666	-2.689980	-2.946148
H	0.310134	-3.670815	-3.313183
H	-1.037060	-2.827904	-2.534479
H	-0.092756	-2.017348	-3.808867
H	2.773606	-2.595854	-2.862613
C	3.212849	-1.194491	-1.271544
H	3.338165	-1.972219	-0.504137
H	2.720344	-0.347504	-0.777051
C	4.590967	-0.757980	-1.784816
H	4.462182	0.030818	-2.540761
H	5.074138	-1.600809	-2.301484
C	5.517017	-0.247508	-0.672990
H	5.023190	0.578998	-0.140475
H	5.662701	-1.044262	0.071970
C	6.885734	0.223197	-1.182193
H	6.740278	1.021738	-1.923654
H	7.376693	-0.602913	-1.716350
C	7.805781	0.726182	-0.064470
H	8.773831	1.055286	-0.459878
H	7.356081	1.574855	0.466041
H	7.997711	-0.061689	0.674727

TS C2-HAT octane (conformation 2) (q)

Fe	-1.012255	0.309889	0.203832
N	0.619168	0.459084	1.393540
N	-1.192337	-1.658124	0.748737
N	-0.853556	2.238656	-0.282162
N	-2.735710	0.181999	-0.810136
C	1.411251	1.566325	1.552120
C	-2.155683	-2.536169	0.329199
C	1.200294	-0.540011	2.141349
C	-0.363795	-2.366585	1.583918
C	0.144993	3.105720	0.096594
C	-3.482300	-0.954052	-1.030871
C	-1.718460	2.972413	-1.058431
C	-3.349798	1.184772	-1.519466
C	2.512273	1.268171	2.435401
C	-1.925990	-3.841546	0.904871
C	2.380046	-0.037940	2.801394
C	-0.815027	-3.734876	1.685633
C	-0.086603	4.411638	-0.477005
C	-4.604984	-0.649066	-1.883442
C	-1.242452	4.330088	-1.189315
C	-4.526128	0.677717	-2.182067
H	3.277834	1.976864	2.724322
H	-2.547630	-4.710052	0.728394
H	3.016081	-0.624882	3.451567
H	-0.333117	-4.498147	2.283171
H	0.559111	5.268174	-0.331327
H	-5.346355	-1.370338	-2.202864
H	-1.745606	5.104605	-1.753924
H	-5.186746	1.272075	-2.800168
C	1.198445	2.801094	0.945653
C	-3.218919	-2.214841	-0.510893
C	-2.888801	2.491959	-1.627915
C	0.750554	-1.851278	2.234060
H	1.908885	3.592285	1.163340
H	-3.908267	-3.012531	-0.769711

H	-3.479356	3.183184	-2.220671
H	1.319475	-2.528666	2.863192
O	-0.059912	-0.134069	-1.203719
S	-2.132961	0.730458	2.247421
C	-3.851490	0.124181	2.164207
H	-3.864871	-0.958852	2.006764
H	-4.324646	0.340870	3.126780
H	-4.409018	0.609052	1.359820
C	1.055487	-2.342489	-1.763616
H	0.433468	-1.232405	-1.347772
H	1.099102	-2.926879	-0.838063
C	2.415430	-1.876476	-2.244682
H	2.281996	-1.142323	-3.052776
C	0.140187	-2.941049	-2.809134
H	0.551469	-3.891696	-3.184103
H	-0.855079	-3.150155	-2.403385
H	0.027855	-2.272140	-3.670841
H	2.932226	-2.736372	-2.707969
C	3.310188	-1.284696	-1.147616
H	3.466441	-2.039607	-0.362895
H	2.783036	-0.448345	-0.670653
C	4.670407	-0.801995	-1.667684
H	4.509851	-0.041228	-2.446169
H	5.191753	-1.636838	-2.159999
C	5.571144	-0.219196	-0.570694
H	5.041787	0.602607	-0.065660
H	5.747530	-0.985041	0.199675
C	6.920707	0.292523	-1.091515
H	6.744234	1.058830	-1.859834
H	7.448870	-0.529042	-1.596451
C	7.814072	0.872014	0.010755
H	8.768678	1.229151	-0.393056
H	7.326238	1.717946	0.511186
H	8.036829	0.118604	0.776767

TS C3-HAT octane (d)

Fe	-0.789816	0.229029	0.241812
N	-1.468056	-1.584596	0.779501
N	-2.461459	0.560060	-0.849650
N	0.778633	-0.009733	1.484066
N	-0.190095	2.131470	-0.165453
C	-0.888426	-2.475221	1.646433
C	-2.761812	1.662947	-1.605822
C	-2.644220	-2.167068	0.377575
C	-3.481591	-0.331979	-1.063154
C	1.072976	-1.104457	2.263062
C	-0.793277	3.036934	-1.003203
C	1.786323	0.895534	1.714072
C	0.971233	2.729776	0.263979
C	-1.705590	-3.657826	1.779391
C	-4.005976	1.466085	-2.312034
C	-2.799277	-3.465160	0.991252
C	-4.455353	0.225909	-1.972388
C	2.293376	-0.883901	3.000010
C	-0.000402	4.242266	-1.094643
C	2.737155	0.357382	2.657836
C	1.094684	4.050550	-0.310064
H	-1.464100	-4.507143	2.405534
H	-4.461103	2.192384	-2.973176
H	-3.642801	-4.124700	0.832349
H	-5.355872	-0.279255	-2.297463
H	2.735446	-1.594519	3.686547
H	-0.263452	5.108835	-1.687629
H	3.620958	0.877577	3.004128
H	1.918550	4.727578	-0.123740
C	0.300873	-2.257432	2.337355

C	-1.991409	2.821941	-1.675123
C	1.890174	2.156557	1.132520
C	-3.574990	-1.593483	-0.483984
H	0.645138	-3.046477	2.998982
H	-2.354935	3.622018	-2.312836
H	2.758786	2.751535	1.398004
H	-4.454704	-2.183405	-0.723182
O	0.060066	-0.281045	-1.229004
S	-1.798551	1.316188	2.208806
C	-3.165237	2.410718	1.698344
H	-3.964960	1.851551	1.206397
H	-3.557518	2.905252	2.592422
H	-2.800543	3.182406	1.011595
C	1.494646	-2.333769	-1.568989
H	0.706719	-1.285623	-1.259397
H	1.544201	-2.842457	-0.597708
C	2.819749	-1.747274	-2.016880
H	2.650599	-1.101094	-2.890762
H	3.448378	-2.578823	-2.383657
C	3.596647	-0.973484	-0.946579
H	3.749697	-1.619039	-0.069431
H	2.988697	-0.128068	-0.604549
C	4.954867	-0.460984	-1.443625
H	4.801084	0.176099	-2.327672
H	5.565286	-1.311279	-1.784096
C	5.736148	0.328819	-0.385253
H	5.126290	1.178964	-0.047862
H	5.889850	-0.305599	0.499443
C	7.090422	0.839284	-0.889364
H	6.965701	1.504235	-1.753204
H	7.734819	0.008207	-1.202525
C	0.760456	-3.127875	-2.632965
H	1.446089	-3.914770	-2.993063
H	0.575861	-2.480967	-3.502142
C	-0.549201	-3.776915	-2.179906
H	-0.982985	-4.381543	-2.984909
H	-0.388058	-4.433845	-1.316697
H	-1.283629	-3.020297	-1.890345
H	7.623066	1.399216	-0.111704

TS C3-HAT octane (q)

Fe	-0.866869	0.367500	0.184050
N	-2.059440	1.354151	-1.077906
N	0.380205	1.932466	0.249001
N	-2.217043	-1.140512	0.305708
N	0.318642	-0.626711	1.526537
C	-3.255575	0.914135	-1.596472
C	1.571401	2.015663	0.936611
C	-1.849742	2.601785	-1.612880
C	0.265856	3.106202	-0.456756
C	-3.401879	-1.228005	-0.377401
C	1.508438	-0.191691	2.045836
C	-2.114529	-2.293772	1.049431
C	0.085918	-1.861602	2.081350
C	-3.798645	1.903001	-2.499573
C	2.209422	3.280696	0.667690
C	-2.928754	2.948576	-2.508944
C	1.400164	3.956968	-0.194549
C	-4.076574	-2.459280	-0.045929
C	2.056312	-1.185561	2.940028
C	-3.277872	-3.119483	0.839386
C	1.174038	-2.222934	2.959814
H	-4.731031	1.794145	-3.038745
H	3.155752	3.592362	1.091070
H	-2.995219	3.879271	-3.057759
H	1.544350	4.938244	-0.628142

H	-5.032817	-2.764682	-0.451118
H	2.990475	-1.081973	3.477175
H	-3.442133	-4.079939	1.310916
H	1.232070	-3.149027	3.517389
C	-3.885650	-0.278209	-1.273416
C	2.098286	1.039261	1.771512
C	-1.042729	-2.641311	1.862235
C	-0.772773	3.427169	-1.322891
H	-4.838688	-0.483861	-1.750493
H	3.048009	1.255390	2.250617
H	-1.097990	-3.595403	2.377003
H	-0.733131	4.393427	-1.815553
O	-0.029922	-0.359316	-1.184101
S	-2.043244	1.085596	2.112950
C	-1.007669	2.211287	3.106756
H	-0.707499	3.091018	2.533192
H	-1.598115	2.518680	3.975438
H	-0.112233	1.692048	3.462108
C	1.369630	-2.458063	-1.498132
H	0.623955	-1.375557	-1.183251
H	1.434938	-2.958042	-0.523534
C	2.700132	-1.930582	-2.001587
H	2.526354	-1.286615	-2.876184
H	3.280221	-2.791216	-2.381141
C	3.548464	-1.179568	-0.969237
H	3.695571	-1.818314	-0.085850
H	2.997802	-0.297096	-0.622306
C	4.914616	-0.745443	-1.516456
H	4.765819	-0.115082	-2.406050
H	5.469641	-1.631422	-1.860517
C	5.767481	0.019281	-0.495573
H	5.212278	0.904601	-0.154101
H	5.916986	-0.609455	0.394017
C	7.129544	0.452002	-1.048988
H	7.011815	1.110005	-1.919053
H	7.720398	-0.415680	-1.368359
C	0.562669	-3.232853	-2.523654
H	1.200078	-4.052916	-2.898227
H	0.372442	-2.589281	-3.394044
C	-0.755320	-3.820158	-2.013336
H	-1.248698	-4.406974	-2.796813
H	-0.587279	-4.481866	-1.155052
H	-1.442951	-3.030387	-1.697932
H	7.714213	0.994786	-0.296994

TS C4-HAT octane (d)

Fe	0.446318	-0.541544	0.294432
N	0.927148	-1.951617	-1.082790
N	-1.302762	-1.484748	0.658203
N	2.275899	0.273195	0.080595
N	-0.000282	0.807811	1.702421
C	2.054141	-1.986391	-1.865029
C	-2.287787	-1.098737	1.531577
C	0.145116	-3.007178	-1.479360
C	-1.756777	-2.628119	0.042678
C	3.227876	-0.074312	-0.849787
C	-1.168707	0.898453	2.426388
C	2.792089	1.334330	0.782490
C	0.824709	1.801641	2.182969
C	1.979920	-3.096277	-2.785081
C	-3.388859	-2.028675	1.477285
C	0.799805	-3.731449	-2.542387
C	-3.058872	-2.976816	0.555944
C	4.377522	0.786097	-0.720173
C	-1.092492	2.003617	3.348686
C	4.112074	1.652410	0.297682

C	0.142881	2.558008	3.202647
H	2.744999	-3.344743	-3.509440
H	-4.288856	-1.949083	2.073296
H	0.392134	-4.608881	-3.027820
H	-3.632423	-3.837570	0.236836
H	5.265458	0.718624	-1.335682
H	-1.886368	2.290665	4.026290
H	4.733742	2.447774	0.688309
H	0.574110	3.397590	3.732633
C	3.128040	-1.111188	-1.767639
C	-2.242150	0.023742	2.347879
C	2.126926	2.044257	1.773885
C	-1.094334	-3.338896	-0.948458
H	3.961960	-1.261936	-2.445472
H	-3.094772	0.214623	2.991157
H	2.657528	2.863610	2.247759
H	-1.592555	-4.214774	-1.351450
O	-0.198603	0.333222	-1.084504
S	1.284577	-2.011255	1.963692
C	3.053352	-2.367193	1.657996
H	3.667066	-1.465996	1.724847
H	3.370373	-3.069714	2.436187
H	3.200397	-2.837246	0.682461
C	-1.381289	2.577141	-1.176906
H	-0.772717	1.484368	-0.996695
H	-1.513342	2.930710	-0.146132
C	-2.693112	2.226338	-1.858143
H	-2.480766	1.738843	-2.820361
H	-3.197580	3.175409	-2.110635
C	-3.651361	1.356493	-1.036987
H	-3.853840	1.847378	-0.073676
H	-3.161603	0.403446	-0.801981
C	-4.978782	1.085173	-1.757946
H	-4.772943	0.586858	-2.716051
H	-5.458973	2.042097	-2.008706
C	-5.947181	0.228261	-0.935577
H	-5.500863	-0.742288	-0.686706
H	-6.209240	0.723423	0.008012
C	-0.452025	3.459110	-1.993537
H	-0.998311	4.390422	-2.224612
H	-0.258237	2.980315	-2.964140
C	0.877053	3.814673	-1.318490
H	0.675684	4.277752	-0.342415
H	1.432001	2.892388	-1.113490
C	1.739085	4.756803	-2.165628
H	2.686343	4.986468	-1.664288
H	1.977134	4.307615	-3.137928
H	1.222876	5.706115	-2.356537
H	-6.878293	0.039805	-1.482712

TS C4-HAT octane (q)

Fe	0.513976	-0.632964	0.202947
N	1.638101	-1.610349	-1.124977
N	-0.992169	-1.919341	-0.104027
N	2.087603	0.544332	0.691504
N	-0.615116	0.342408	1.607699
C	2.940368	-1.330178	-1.469352
C	-2.245094	-1.881365	0.467540
C	1.268029	-2.691786	-1.887739
C	-1.012870	-2.962483	-0.997748
C	3.332073	0.518385	0.117971
C	-1.911720	0.066398	1.951267
C	2.111748	1.561204	1.619111
C	-0.227279	1.401426	2.391128
C	3.391355	-2.245663	-2.492391
C	-3.064563	-2.939808	-0.069143

C	2.356387	-3.089420	-2.750676
C	-2.300756	-3.610554	-0.976309
C	4.172406	1.531562	0.707818
C	-2.366726	0.989528	2.965276
C	3.415535	2.177008	1.639527
C	-1.321245	1.819206	3.236653
H	4.379381	-2.231958	-2.934462
H	-4.090571	-3.128025	0.220367
H	2.314147	-3.914351	-3.450265
H	-2.569290	-4.462439	-1.587823
H	5.202648	1.713541	0.429755
H	-3.356208	0.982643	3.404300
H	3.695283	3.000525	2.284014
H	-1.272686	2.635832	3.945643
C	3.733005	-0.347628	-0.895689
C	-2.676813	-0.968450	1.420750
C	1.039512	1.972181	2.400487
C	0.038406	-3.331139	-1.829482
H	4.750831	-0.250984	-1.260100
H	-3.695095	-1.071775	1.782219
H	1.208465	2.801634	3.080058
H	-0.118739	-4.178808	-2.488853
O	-0.032188	0.451317	-1.071604
S	1.324378	-1.873031	2.050699
C	0.007423	-2.926210	2.746394
H	-0.385009	-3.623397	2.002847
H	0.441703	-3.482572	3.582843
H	-0.812241	-2.309740	3.128279
C	-1.125988	2.745505	-1.117039
H	-0.565827	1.529103	-0.943990
H	-1.259625	3.062818	-0.075212
C	-2.432435	2.522855	-1.855730
H	-2.224296	2.042800	-2.823147
H	-2.849503	3.515716	-2.104281
C	-3.493729	1.716885	-1.098465
H	-3.672892	2.181064	-0.117320
H	-3.108439	0.710133	-0.896813
C	-4.822417	1.608425	-1.858437
H	-4.639520	1.153739	-2.842570
H	-5.212633	2.617298	-2.056106
C	-5.878576	0.789665	-1.108260
H	-5.526828	-0.233494	-0.926012
H	-6.109602	1.239290	-0.134260
C	-0.096532	3.564959	-1.872484
H	-0.552785	4.543156	-2.110133
H	0.101877	3.090024	-2.844593
C	1.227029	3.801192	-1.136827
H	1.022042	4.268231	-0.163418
H	1.692992	2.833053	-0.923285
C	2.200697	4.678647	-1.930690
H	3.140704	4.821272	-1.385203
H	2.443211	4.223547	-2.899267
H	1.774487	5.670415	-2.128415
H	-6.814220	0.725295	-1.675910

1. References

- 1 P. Püllmann, C. Ulpinnis, S. Marillonnet, R. Gruetzner, S. Neumann and M. J. Weissenborn, *Sci. Rep.*, 2019, **9**, 10932.
- 2 S. Kille, C. G. Acevedo-Rocha, L. P. Parra, Z.-G. Zhang, D. J. Opperman, M. T. Reetz and J. P. Acevedo, *ACS Synth. Biol.*, 2013, **2**, 83–92.
- 3 C. G. Acevedo-Rocha, M. T. Reetz and Y. Nov, *Sci. Rep.*, 2015, **5**, 10654.
- 4 a) M. K. Tse, M. Klawonn, S. Bhor, C. Döbler, G. Anilkumar, H. Hugl, W. Mägerlein and M. Beller, *Org. Lett.*, 2005, **7**, 987–990; b) F. G. Delolo, E. N. dos Santos and E. V. Gusevskaya, *Green Chem.*, 2019, **21**, 1091–1098;
- 5 M. Constantino, V. Lacerda and V. Aragão, *Mol.*, 2001, **6**, 770–776.
- 6 M. J. Frisch, G. W. Trucks, H. B. Schlegel, G. E. Scuseria, M. A. Robb, J. R. Cheeseman, G. Scalmani, V. Barone, G. A. Petersson, H. Nakatsuji, X. Li, M. Caricato, A. V. Marenich, J. Bloino, B. G. Janesko, R. Gomperts, B. Mennucci, H. P. Hratchian, J. V. Ortiz, A. F. Izmaylov, J. L. Sonnenberg, Williams, F. Ding, F. Lipparini, F. Egidi, J. Goings, B. Peng, A. Petrone, T. Henderson, D. Ranasinghe, V. G. Zakrzewski, J. Gao, N. Rega, G. Zheng, W. Liang, M. Hada, M. Ehara, K. Toyota, R. Fukuda, J. Hasegawa, M. Ishida, T. Nakajima, Y. Honda, O. Kitao, H. Nakai, T. Vreven, K. Throssell, J. A. Montgomery Jr., J. E. Peralta, F. Ogliaro, M. J. Bearpark, J. J. Heyd, E. N. Brothers, K. N. Kudin, V. N. Staroverov, T. A. Keith, R. Kobayashi, J. Normand, K. Raghavachari, A. P. Rendell, J. C. Burant, S. Iyengar, J. Tomasi, M. Cossi, J. M. Millam, M. Klene, C. Adamo, R. Cammi, J. W. Ochterski, R. L. Martin, K. Morokuma, O. Farkas, J. B. Foresman and D. J. Fox, *Gaussian 16 Rev. C.01*, Wallingford, CT, 2016.
- 7 a) Lee, Yang and Parr, *PRB*, 1988, **37**, 785–789; b) A. D. Becke, *J. Chem. Phys.*, 1993, **98**, 5648–5652; c) Becke, *PRA*, 1988, **38**, 3098–3100;
- 8 a) Y. Zhao and D. G. Truhlar, *Phys. Chem. Chem. Phys.*, 2008, **10**, 2813–2818; b) R. F. Ribeiro, A. V. Marenich, C. J. Cramer and D. G. Truhlar, *J. Phys. Chem. B*, 2011, **115**, 14556–14562;
- 9 I. Funes-Ardoiz and R. S. Paton, *Goodvibes: Goodvibes V1.0.1*, Zenodo, 2016.
- 10 a) M. Cossi, N. Rega, G. Scalmani and V. Barone, *J. Comp. Chem.*, 2003, **24**, 669–681; b) V. Barone and M. Cossi, *J. Phys. Chem. A*, 1998, **102**, 1995–2001;
- 11 C. N. Schutz and A. Warshel, *Proteins*, 2001, **44**, 400–417.
- 12 S. Grimme, S. Ehrlich and L. Goerigk, *J. Comp. Chem.*, 2011, **32**, 1456–1465.
- 13 A. Knorrscheidt, J. Soler, N. Hünecke, P. Püllmann, M. Garcia-Borràs and M. Weissenborn, *Accessing Chemo- and Regioselective Benzylic and Aromatic Oxidations by Protein Engineering of an Unspecific Peroxygenase*, 2020.
- 14 V. W. D. Cruzeiro, M. S. Amaral and A. E. Roitberg, *J. Chem. Phys.*, 2018, **149**, 72338.
- 15 P. Li and K. M. Merz, *J. Chem. Info. Model.*, 2016, **56**, 599–604.
- 16 J. Wang, R. M. Wolf, J. W. Caldwell, P. A. Kollman and D. A. Case, *J. Comp. Chem.*, 2004, **25**, 1157–1174.
- 17 C. I. Bayly, P. Cieplak, W. Cornell and P. A. Kollman, *J. Phys. Chem.*, 1993, **97**, 10269–10280.
- 18 a) U. C. Singh and P. A. Kollman, *J. Comp. Chem.*, 1984, **5**, 129–145; b) B. H. Besler, K. M. Merz and P. A. Kollman, *J. Comp. Chem.*, 1990, **11**, 431–439;
- 19 K. Shahrokh, A. Orendt, G. S. Yost and T. E. Cheatham, *J. Comp. Chem.*, 2012, **33**, 119–133.
- 20 W. L. Jorgensen, J. Chandrasekhar, J. D. Madura, R. W. Impey and M. L. Klein, *J. Chem. Phys.*, 1983, **79**, 926–935.
- 21 J. A. Maier, C. Martinez, K. Kasavajhala, L. Wickstrom, K. E. Hauser and C. Simmerling, *J. Chem. Theory Comput.*, 2015, **11**, 3696–3713.

- 22 T. Darden, D. York and L. Pedersen, *J. Chem. Phys.*, 1993, **98**, 10089–10092.
- 23 D. R. Roe and T. E. Cheatham, *J. Chem. Theory Comput.*, 2013, **9**, 3084–3095.
- 24 O. Trott and A. J. Olson, *J. Comp. Chem.*, 2010, **31**, 455–461.